รายงานวิจัยฉบับสมบูรณ์

โครงการ การทำแห้งผลิตภัณฑ์อาหารโดยใช้ไอน้ำร้อนยวดยิ่งที่สภาวะความดันต่ำ

โดย ผศ. ดร. สักกมน เทพหัสดิน ณ อยุธยา

มิถุนายน พ.ศ. 2547

สัญญาเลขที่ TRG4580099

รายงานวิจัยฉบับสมบูรณ์

โครงการ การทำแห้งผลิตภัณฑ์อาหารโดยใช้ไอน้ำร้อนยวดยิ่งที่สภาวะความดันต่ำ

ผู้วิจัย

ผศ. ดร. สักกมน เทพหัสดิน ณ อยุธยา

สังกัด

มหาวิทยาลัยเทคโนโลยีพระจอมเกล้าธนบุรี

สนับสนุนโดยสำนักงานกองทุนสนับสนุนการวิจัย

Acknowledgements

First of all, the investigator would like to express his sincere appreciation to the Thailand Research Fund (TRF) and the International Foundation for Science (Sweden) for supporting this study financially.

The investigator would also like to acknowledge the support and guidance from his mentor, Prof. Somchart Soponronnarit of the School of Energy and Materials, KMUTT. The suggestions and advices of Prof. Arun S. Mujumdar of the Mechanical Engineering Department, National University of Singapore are also appreciated. The assistance provided by my doctoral student, Ms. Peamsuk Suvarnakuta of the Food Engineering Department, KMUTT, as well as by the supporting staff of the department is also gratefully acknowledged.

รหัสโครงการ: TRG4580099

ชื่อโครงการ: การทำแห้งผลิตภัณฑ์อาหารโดยใช้ไอน้ำร้อนยวดยิ่งที่สภาวะความดันต่ำ

ชื่อนักวิจัย: ผศ.ดร.สักกมน เทพหัสดิน ณ อยุธยา

E-mail Address: sakamon.dev@kmutt.ac.th

ระยะเวลาโครงการ: 2 ปี

บทคัดย่อ

งานวิจัยนี้ศึกษาการทำแห้งผลิตภัณฑ์อาหารโดยใช้ไอน้ำร้อนยวดยิ่งที่สภาวะความดันต่ำ ซึ่งเป็นทางเลือกใหม่ในการทำแห้งผลิตภัณฑ์อาหารที่เปลี่ยนแปลงได้ง่ายเมื่อได้รับความร้อน เช่น ผักและผลไม้ โดยได้ทำการออกแบบ สร้าง และทดสอบเครื่องทำแห้งต้นแบบที่ใช้ไอน้ำร้อนยวดยิ่งที่สภาวะความดันต่ำเป็นตัวกลางในการทำแห้ง และทำการศึกษาผลของสภาวะการทำแห้งต่างๆ ที่มีต่อจลนศาสตร์การทำแห้งและคุณภาพด้านต่างๆ ของผลิตภัณฑ์ที่ผ่านกระบวนการดังกล่าว และเปรียบเทียบกับผลที่ได้จากการทำแห้งด้วยกระบวนการอื่นด้วย

ในส่วนแรกของงานวิจัยเป็นการศึกษาการทำแห้งแครอท โดยทำการศึกษาผลของสภาวะการทำแห้งต่างๆ ที่มีต่อจลนศาสตร์การทำแห้งและคุณภาพต่างๆ คือ ปริมาตร การหดตัว ความหนาแน่นปรากฏ สี และการคืนตัวของแครอท และเปรียบเทียบผลที่ได้กับผลการทำแห้งโดยใช้ระบบการทำแห้งแบบสุญญากาศ จากผลที่ได้พบว่า ถึงแม้ว่าจะต้องใช้เวลามากกว่าในการทำแห้งแครอทโดยใช้ไอน้ำร้อนยวดยิ่งที่สภาวะความดันต่ำ เมื่อเปรียบเทียบกับกรณีการใช้ระบบทำแห้งแบบสุญญากาศ แต่แครอทแห้งที่ได้มีความสามารถในการคืนตัว และสีที่ดีกว่าผลิตภัณฑ์ที่ผ่านการทำแห้งด้วยระบบการทำแห้งแบบสุญญากาศ ซึ่งเป็นกระบวนการทำแห้งที่ยอมรับกันโดยทั่วไปว่าให้ผลิตภัณฑ์ที่มีคุณภาพดีวิธีการหนึ่ง

จากผลงานวิจัยในส่วนแรกพบว่า เมื่อใช้อุณหภูมิทำแห้งสูงขึ้น ผลต่างของเวลาการทำแห้งระหว่างกรณีการใช้ไอน้ำร้อนยวดยิ่งที่สภาวะความดันต่ำกับการใช้ระบบสุญญากาศมีค่าลดลง ดังนั้นงานวิจัยในส่วนที่สองจึงได้ทำการศึกษาเพิ่มเติมถึงอัตราการทำแห้งของระบบการทำแห้งที่ใช้ไอน้ำร้อนยวดยิ่ง และระบบสุญญากาศที่อุณหภูมิและความดันต่างๆ รวมทั้งศึกษาผลของความดันที่มีต่อค่าอุณหภูมิผกผันโดยใช้ molecular sieve beads เป็นวัสดุทดสอบ จากการศึกษาพบว่าค่าอุณหภูมิผกผันที่คำนวณได้เฉพาะจากช่วงอัตราการทำแห้งคงที่ มีค่าแตกต่างจากค่าอุณหภูมิผกผันที่คำนวณได้จากช่วงการทำแห้งโดยรวมทั้งหมด นอกจากนี้ยังพบด้วยว่าสมการของ Page สามารถทำนายการเปลี่ยนแปลงค่าความชื้นของผลิตภัณฑ์ที่ผ่านการทำแห้งโดยใช้ไอน้ำร้อนยวดยิ่งที่สภาวะความดันต่ำได้ดี ในขณะที่สมการแบบ Single-term exponential สามารถทำนายผลการทำแห้งภายใต้ระบบสุญญากาศได้ดี

คำหลัก: คุณภาพ; แครอท; สมการเอมไพริเคิล; อัตราการทำแห้ง; molecular sieves

Project Code: TRG4580099

Project Title: Low-pressure superheated steam drying of food products

Investigator: Ass. Prof. Dr. Sakamon Devahastin

E-mail Address: sakamon.dev@kmutt.ac.th

Project Period: 2 years

Abstract

The present research aimed at studying drying of some food products in a low-pressure superheated steam drying system, which is proposed as an alternative for drying heat-sensitive food products, e.g., fruits and vegetables. The project involved the design, fabrication and testing of a cabinet-type low-pressure superheated steam dryer prototype as well as the investigation of the effects of various drying parameters on the drying kinetics and quality of a food product undergoing this drying operation. The results obtained were also compared with those obtained using other type of drying process as well.

In the first part of the study carrot cubes were used as the test materials to determine the effects of various drying parameters on their drying kinetics and various quality attributes, i.e., volume, shrinkage, apparent density, color and rehydration behavior. The results obtained were compared with a similar set of results obtained from a vacuum drying system. It was found that although low-pressure superheated steam drying required longer dwell time to achieve the same final moisture content than that of vacuum drying, some of the quality attributes, especially color and rehydration behavior of the dried carrot, were superior to those obtained in vacuum drying.

Based on the results of the first part it was observed that the differences between the two sets of drying times (low-pressure superheated steam and vacuum drying) were smaller at higher drying temperatures. The second part of the study thus aimed to further investigate the rates of both low-pressure superheated steam and vacuum drying at various temperatures and pressures. The effect of operating pressure on the value of an inversion temperature was also investigated in this part of the study. Molecular sieve beads were used as the test materials in this part. From the study it was found that the values of the inversion temperature calculated only from the rates of drying in the constant rate period were different from those calculated from the whole drying period (constant rate period and falling rate period). Page's equations and a single-term exponential equation were found to satisfactorily describe the kinetics of low-pressure superheated steam drying and vacuum drying system, respectively.

Keywords: carrot; drying rate; empirical models; molecular sieves; qualities

Contents

Research Results

Module 1

A Comparative Study of Low-pressure Superheated Steam and Vacuum Drying of Carrot Cubes

1.1 Introduction

Currently, a majority of dryers in the food industry are of direct (or convective) type and use hot air as the drying medium. During the past decade, however, the idea of using superheated steam to dry foods has been derived from other industries (e.g., paper and wood industries). The process involves the use of superheated steam (instead of hot air) as the drying medium in a direct dryer to supply heat for drying and to carry away the evaporated moisture. Any direct or direct/indirect (e.g., combined conduction/convection) dryer can be operated as a superheated steam dryer, at least in principle. The technology involved is more complex (and more expensive) and hence this conversion is not simple, however.

Although one of the most obvious advantages of superheated steam drying (SSD), i.e., the ability to recover all of the latent heat supplied to the dryer by condensing the exhaust steam or by mechanical or thermal compression to elevate its specific enthalpy for reuse in the dryer may not be of utmost interest to the food processors, its other advanthages, as summarized below, are much more attractive.

Generally, no oxidative reactions (e.g., enzymatic browning, lipid oxidations) are possible in SSD due to lack of oxygen. This is especially beneficial when browning is not desirable, e.g., during drying of apple and banana. In addition, higher drying rates, compared to air drying, are possible in both constant and falling rate periods of SSD, depending on the steam temperature. Also, it is known that many food products that form casehardened skin in rapid drying do not form such water-impermeable skin in SSD (Mujumdar, 2000). Another noted advantage of SSD is that, for certain foods or vegetables, the porosity of the products dried in superheated steam is higher than that dried in hot air (Li et al., 1998). This is due to the evolution of steam within the product. This decreases bulk density of the product while enhancing its rehydration characteristics. This feature is especially attractive for the instant foods as well as confectionary industries.

Several limitations, which partly prevent SSD from being widely used in the food industry, are still presented, however. Products that may melt, undergo glass transition or be

damaged at the saturation temperature of steam at the dryer operating pressure cannot clearly be dried in superheated steam dryer even if they contain only surface moisture. One possible way to prevent the products from being damaged in a high-temperature environment of SSD is to operate a dryer at reduced pressure. Since the boiling point of water, which obviously related to the product temperature, decreases with pressure, it is possible to operate the dryer at a temperature lower than a maximum permissible temperature of the product of interest. The drying rate may be enhanced in a low-pressure operation as well.

At present, there is a very limited experience with the low-pressure superheated steam drying, especially when considering the process from product quality point of view. One of the objectives of the present research project is thus to study low-pressure SSD, especially from the dried product quality point of view, which is generally unpredictable a priori, and make it more suitable and widely acceptable in the food industry.

1.2 Objectives

1.2.1 To design, fabricate and test the cabinet-type low-pressure superheated steam dryer prototype

1.2.2 To investigate the influences of various operating parameters (i.e., steam temperature and pressure) on the drying characteristics (e.g., drying curves and product temperature profiles) as well as on the various quality attributes of a selected food product and compare the results with those obtained using other drying technique viz. vacuum drying system

1.3 Experimental Set-up

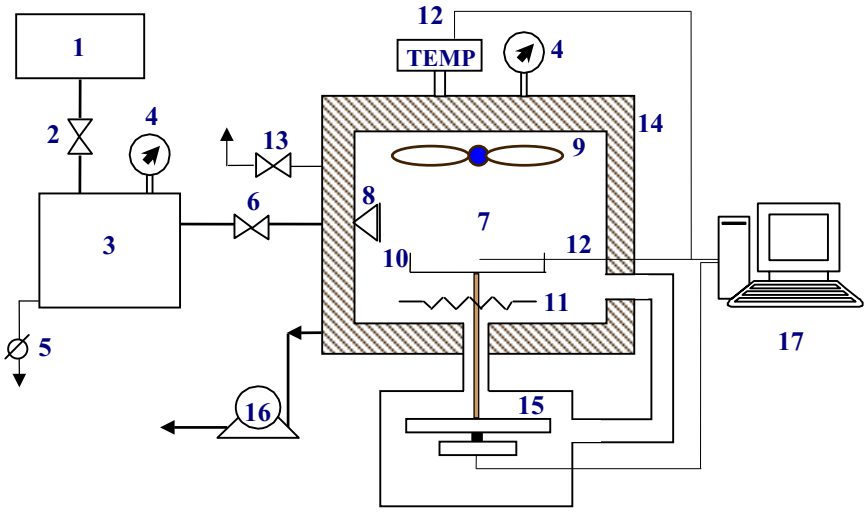

Figure 1. A schematic diagram of the low-pressure superheated steam dryer and associated units. 1, boiler; 2, steam valve; 3, steam reservoir; 4, pressure gauge; 5, steam trap; 6, steam regulator; 7, drying chamber; 8, steam inlet and distributor; 9, electric fan; 10, sample holder; 11, electric heater; 12, on-line temperature sensor and logger; 13, vacuum break-up valve; 14, insulator; 15, on-line weight indicator and logger; 16, vacuum pump; 17, PC with installed data acquisition card

A schematic diagram of the low-pressure superheated steam dryer and its accessories is shown in Figure 1. The dryer consists of a stainless steel drying chamber, insulated carefully with rock wool, with an inner dimension of $45\times 45\times 45$ cm^3; a steam reservoir, which received the steam from the boiler and maintained its pressure at around 200 kPa (gage); and a liquid ring vacuum pump (Nash, model ET32030, Germany), which was used to maintain the vacuum in the drying chamber. Steam trap was installed to reduce the excess steam condensation in the reservoir. An electric heater, rated at 1.5 kW, which was controlled by a PID controller (Omron, model E5CN, Japan) was installed in the drying chamber to control the steam temperature and to minimize the condensation of steam in the drying chamber during the start-up period; with the use of a heater the initial steam condensation during the start-up period was reduced considerably. A variable-speed electric fan was used to disperse steam throughout the drying chamber. The steam inlet was made into a cone shape and was covered with a screen to also help distributing the steam in the chamber. The sample holder was made of a stainless steel screen with a dimension of 12×12 cm^2. The change of the weight of the sample was detected continuously (at 30 seconds intervals) using a load cell (Minebea, model Ucg-3kg, Japan), which was installed in a smaller chamber connected to the drying chamber by a flexible hose

(in order to maintain the same vacuum pressure as that in the drying chamber), and also to an indicator and recorder (AND A&D Co., model AD 4329, Japan). The temperatures of the steam and of the drying sample were also measured continuously using type K thermocouples, which were connected to an expansion board (Omega Engineering, model no. EXP-32, USA). Thermocouple signals were then multiplexed to a data acquisition card (Omega Engineering, model no. CIO-DAS16Jr., USA) installed in a PC. LABTECH NOTEBOOK software (version 12.1, Laboratory Technologies Corp., USA) was then used to read and record the temperature data.

1.4 Material and Methods

Fresh carrot was obtained from a local supermarket and stored at 4°C. Prior to the start of each experiment carrot was peeled and diced into 1 cm^3 cubes. To perform a drying experiment approximately 35 cubes of carrot (about 40 g) were placed on the sample holder. The drying chamber was then sealed tightly. Valve 2 was opened to allow the steam from the boiler to flow into the reservoir; the steam pressure was maintained at about 200 kPa (gage) in the reservoir. A vacuum pump was then switched on to evacuate the drying chamber to the desired operating pressure and the steam regulator was opened to slowly flash the steam into the drying chamber. Due to the low-pressure environment of the chamber the steam became superheated. An electric heater was used to maintain the steam temperature at a desired drying temperature. At the end of the drying process the break-up valve was opened to allow the air into the drying chamber (to regain an atmospheric condition) before opening up the chamber door and loading off the dried product.

For vacuum drying experiments the same experimental set-up was used but without the application of steam to the drying chamber. The same operating conditions were therefore achievable. The experiments were performed at the following conditions: steam absolute pressures of 7, 10 and 13 kPa; steam temperatures of 60°, 70° and 80°C. The flow rate of steam into the drying chamber (in the case of SSD) was maintained at about 26 kg/h and the speed of the fan was fixed at 2100 rpm.

1.5 Results and Discussion

1.5.1 Drying characteristics of carrot Cubes

After the low-pressure superheated steam dryer was fabricated it was tested to ensure that the distribution of the steam temperature within the drying chamber was uniform. It was found from this study that the maximum difference of the steam temperature within the drying

chamber was within ±3°C. The dryer was then used to conduct both low-pressure superheated steam drying (LPSSD) and conventional vacuum drying experiments.

Carrot that had an initial moisture content of about 9 kg/kg (d.b.) was dried to a final moisture content of about 0.07 kg/kg (d.b.) in the dryer using both low-pressure superheated steam and conventional vacuum drying. The drying curves of carrot undergoing LPSSD are shown in Figure 2; a slight decrease in the moisture content during the first 5 minutes of the process was due to the initialization of the chamber pressure and of the load cell. Drying indeed started at about 5 minutes after the weight was initially recorded. It can be seen in this figure that all samples gained a small amount of moisture during the first few minutes of drying (after the above-mentioned 5 minutes) for all drying conditions due to steam condensation. This phenomenon is indeed typical of superheated steam drying (e.g., Tang et al., 2000; Mujumdar, 2000) although, in this study, the drying chamber was preheated at 50°C during the first 5 minutes of the process. Nevertheless, the condensation of steam was rather negligible if the operating pressure was low; for example, the samples gained moisture of about 1.4%, 1.3% and 1 % when drying at 60°, 70° and 80°C at 7 kPa, respectively. Accordingly, the restoration time, which is the time by which the original mass has returned to its original value (Iyota et al., 2001) was 5, 4 and 4 minutes for drying at 60°, 70° and 80°C at 7 kPa, respectively.

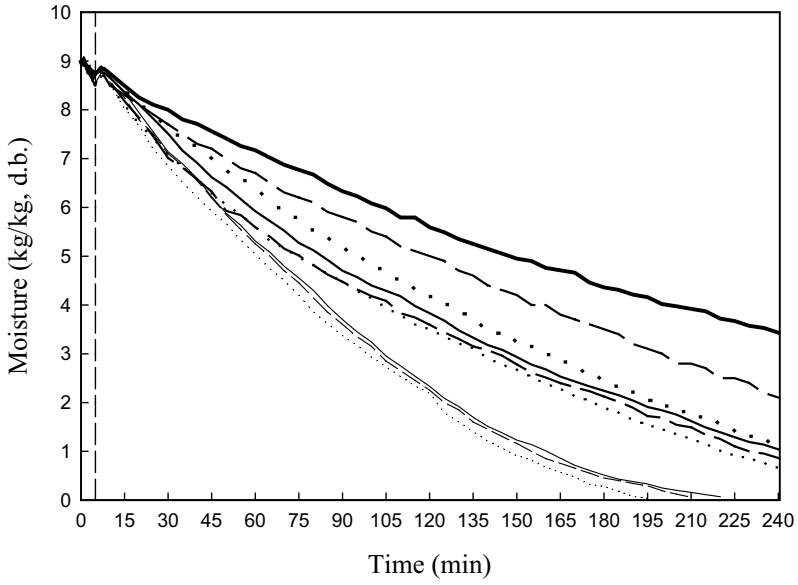

Figure 2. Drying curves of carrot undergoing LPSSD during the first 4 hours of experiments (Legends used are the same as in Figure 3).

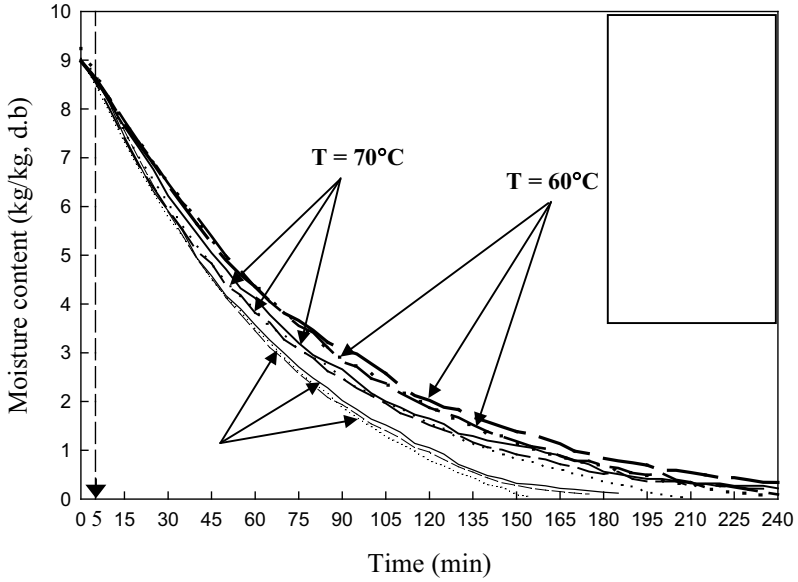

Figure 3. Drying curves of carrot undergoing vacuum drying during the first 4 hours of experiments.

Table 1 lists the drying times of all LPSSD and vacuum drying experiments. It can be seen from this table and also from Figure 2 that the effect of temperature on the drying rates was greater than the effect of pressure in the case of LPSSD, especially at higher drying temperatures. The effect of operating pressure was less clear even at lower temperature (60°C) for the case of vacuum drying, as can be seen in Figure 3, however. This may probably due to the fact that the steam thermal properties were affected by temperature to a larger extent than those of air, especially at lower drying temperatures. No initial condensation was also observed, as expected, in the case of vacuum drying. It can also be seen that the moisture decreased faster at a higher temperature than at a lower temperature because the temperature difference between the sample and the medium at a higher drying temperature was greater than that at a lower temperature. For example, an increase of the drying temperature from 60°C to 80°C led to a reduction in the drying time of about 49% and 32% in the case of LPSSD and vacuum drying at an operating pressure of 7 kPa, respectively. In addition, it was observed that the moisture content decreased faster, especially in the case of LPSSD at lower drying temperatures, at lower pressures since water in carrot boiled and evaporated at lower temperatures; a decrease of the pressure from 13 kPa to 7 kPa, for example, led to a reduction of the drying time by 14% and 23% in the case of LPSSD and vacuum drying at a temperature of 80°C, respectively. Performing LPSSD experiments at higher pressures and lower temperatures also led to another problem, i.e., it was not able to dry carrot to the required

moisture content of 0.07 kg/kg (d.b.) because there was an excessive amount of steam condensation in the drying chamber.

Table 1. Average drying times of LPSSD and vacuum drying of carrot at various operating conditions.

Drying time of LPSSD (min)			
Pressure (kPa)	Temperature (°C)		
	60	70	80
7	389	280	198
10	N/A	290	210
13	N/A	317	230
Drying time of vacuum drying (min)			
Pressure (kPa)	Temperature (°C)		
	60	70	80
7	235	205	159
10	241	223	175
13	255	265	206

N/A implies that, at this condition, the final carrot moisture content of 0.07 kg/kg (d.b.) was not achievable

It was found that the drying times of vacuum drying were shorter than those of LPSSD (at the same pressure) for all conditions tested. This is probably due to the fact that the electric heater was used more often during vacuum drying since it was the only source of energy for drying. This might increase the amount of radiation absorbed by the carrot surfaces, thus explaining the higher drying rate during vacuum drying. The initial steam condensation on the product surface might also contribute to the longer drying times for the case of LPSSD. The differences between the two sets of drying times, however, were smaller at higher drying temperatures. Raising the drying temperature further would eventually lead to equal rates of drying at an inversion temperature (due to increased temperature difference between the steam and the product as well as a reduction of the initial steam condensation). This could not be done in this case, however, as it would adversely affect the quality of the dried carrot.

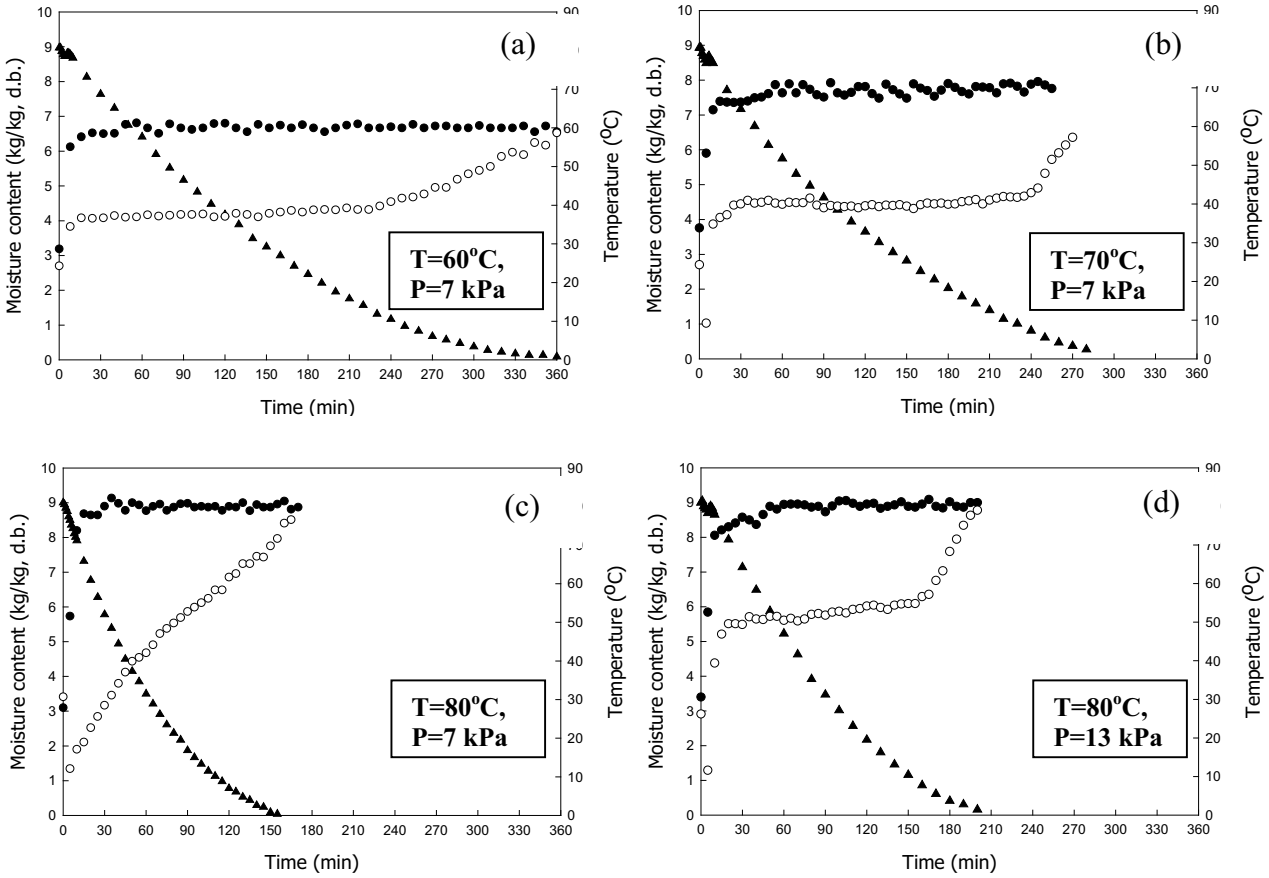

Figure 4. Changes in moisture content and temperature of carrot undergoing LPSSD at different operating conditions. ▲ moisture content; ● steam temperature; ○ sample temperature

Figure 4 illustrates changes of moisture content and temperature of carrot undergoing LPSSD at some selected conditions. It can be seen in this figure that the shapes of the drying and temperature curves were affected by both the drying temperature and pressure. At lower drying temperatures (say, at 60°C and 70°C) the temperature of carrot changed suddenly from its initial value (after initial adjustment) and remained rather constant at the boiling temperature of water corresponding to the operating pressure until the first falling rate period drying ended (drying rate data are not shown here for the sake of brevity). Beyond this point, the carrot temperature rose again and finally approached the temperature of the drying medium. As the medium temperature increased (at the same operating pressure) it can be seen (for example, from Figure 4c) that the period of constant product temperature was shorter; the product temperature rose almost steadily from its initial value to the medium temperature. At the same drying temperature, however, increasing of the operating pressure led to a lower rate of drying but a longer period of constant product temperature (as can be seen from Figures 4c and 4d). It

may depend both on the characteristics of the drying product and on these effects to determine the optimum operating conditions of an LPSSD.

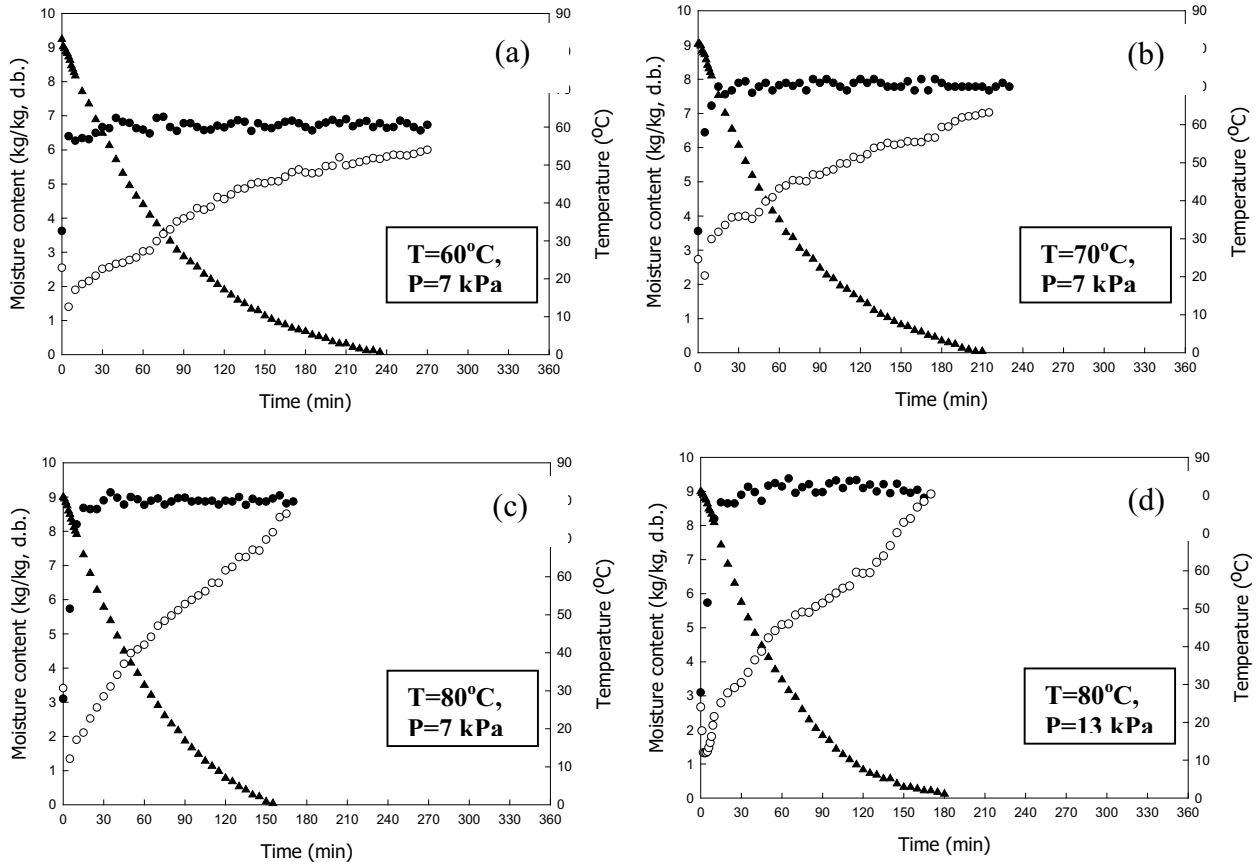

Figure 5. Changes in moisture content and temperature of carrot undergoing vacuum drying at different operating conditions. ▲ moisture content; ● steam temperature; ○ sample temperature

Figure 5 shows the evolutions of moisture content and temperature of carrot undergoing vacuum drying at the same operating as those used for LPSSD shown in Figure 4. It can be seen from this figure that the drying and heat transfer behavior of carrot undergoing vacuum drying was quite different from that of LPSSD; the product temperature, in this case, rose almost steadily from its initial value to the medium temperature. However, the rates of moisture reduction in the case of vacuum drying were higher than those belonged to LPSSD, especially at lower drying temperatures as mentioned earlier. Attempts were also made to compare the present data with a similar set of data available in the literature, i.e., the processes of freeze drying, air drying and microwave vacuum drying of carrot, in terms of the average drying rates over the whole period of drying (Lin et al., 1998). It was found that the lowest drying rates obtained in the present study (which corresponded to using LPSSD at 60°C and 7 kPa) of 1.38 kg water kg^{-1} dry matter h^{-1} was, as expected, lower than that achievable by microwave vacuum

drying (19.1 kg water kg^{-1} dry matter h^{-1}) but was still higher than those obtained by air drying and freeze drying of blanched carrot slices (1.31 and 0.013 kg water kg^{-1} dry matter h^{-1}, respectively). It should be noted that it is easier to dry blanched carrot than fresh carrot used in the present study. The carrot slices used by Lin et al. (1998) also had less thickness (4 mm) than that used in our study as well.

1.5.2 Qualities of carrot cubes

Table 2 illustrates the effects of the drying temperature and pressure of both LPSSD and vacuum drying on various physical properties of carrot, i.e., volume, density, shrinkage and rehydration behavior. It was found that the volume of dried carrot was inversely proportional to its apparent density; carrot that had lower apparent density has larger volume, as expected. It can be seen also that the volume and apparent density of dried carrot undergoing both drying techniques slightly decreased and increased, respectively, as the operating pressure increased. This is due to the fact that pressure affects the percentage of air pores developed in the final dried products (Krokida and Maroulis, 2000); both properties changed only slightly in this case, however, because the narrow range of operating pressures tested. Different drying techniques as well as the drying temperature also did not have much effect on the volume and density of the final dried products in this case. This is in accordance with the results reported by Krokida et al. (1997) who compared the apparent density of dried carrot and other dried food products undergoing convective hot-air, microwave, freeze and osmotic drying; it was found in their work that the operating pressure significantly affected the apparent density of the dried products than did the other operating parameters. Lowering the pressure during subatmospheric drying (both LPSSD and vacuum drying) also helped preventing the structural collapse of foods, especially in the case of carrot.

Table 2. Physical properties of carrot undergoing LPSSD and vacuum drying at different drying conditions.

Drying Process	Temperature (°C)	Pressure (kPa)	Volume (cm^3)	Density (g/cm^3)	Shrinkage (%)	Rehydration ratio
LPSSD	T = 60°C	7	0.092 ± 0.002^{d}	1.43 ± 0.03^{a}	90.80 ± 0.09^{ab}	5.19 ± 0.08^{f}
		10	N/A	N/A	N/A	N/A
		13	N/A	N/A	N/A	N/A
	T = 70°C	7	0.092 ± 0.008^{d}	1.42 ± 0.02^{a}	90.77 ± 0.09^{a}	5.21 ± 0.09^{fg}
		10	0.087 ± 0.01^{a}	1.50 ± 0.04^{d}	91.21 ± 0.07^{de}	5.10 ± 0.14^{de}
		13	0.086 ± 0.004^{a}	1.51 ± 0.06^{de}	91.23 ± 0.10^{gh}	4.94 ± 0.04^{d}
	T = 80°C	7	0.093 ± 0.009^{c}	1.43 ± 0.11^{ab}	90.8 ± 0.09^{ab}	5.23 ± 0.15^{h}
		10	0.09 ± 0.006^{b}	1.44 ± 0.01^{b}	90.82 ± 0.06^{b}	5.19 ± 0.05^{f}
		13	0.088 ± 0.008^{ab}	1.45 ± 0.08^{c}	91.09 ± 0.02^{f}	5.15 ± 0.07^{e}
Vacuum drying	T = 60°C	7	0.092 ± 0.009^{c}	1.42 ± 0.1^{ab}	90.85 ± 0.11^{cd}	4.39 ± 0.18^{b}
		10	0.09 ± 0.012^{b}	1.43 ± 0.04^{ab}	90.97 ± 0.14^{d}	4.17 ± 0.16^{a}
		13	0.09 ± 0.007^{b}	1.43 ± 0.03^{ab}	90.99 ± 0.08^{d}	4.10 ± 0.04^{a}
	T = 70°C	7	0.092 ± 0.003^{c}	1.43 ± 0.07^{ab}	90.82 ± 0.04^{b}	4.51 ± 0.03^{bc}
		10	0.091 ± 0.004^{bc}	1.40 ± 0.09^{a}	91.08 ± 0.04^{ef}	4.47 ± 0.09^{c}
		13	0.091 ± 0.01^{bc}	1.43 ± 0.02^{ab}	90.93 ± 0.05^{d}	4.13 ± 0.07^{b}
	T = 80°C	7	0.092 ± 0.002^{e}	1.42 ± 0.04^{ab}	90.79 ± 0.04^{a}	4.82 ± 0.04^{de}
		10	0.092 ± 0.009^{c}	1.42 ± 0.12^{ab}	90.82 ± 0.11^{b}	4.56 ± 0.15^{c}
		13	0.09 ± 0.009^{b}	1.42 ± 0.07^{ab}	90.95 ± 0.09^{d}	4.51 ± 0.13^{c}

Table 2 also shows the results of shrinkage of carrot undergoing different drying techniques and operating conditions. Like the apparent density, shrinkage values correlated directly with the volume of dried carrot. It can be seen from Table 2 that the percentage of shrinkage of LPSSD and vacuum dried carrot was similar although superheated steam drying is known to have a potential to reduce the degree of shrinkage of the drying product due to an evolution of vapor inside the product that expands into cells, leading to a normally porous dried product (Seyed-Yagoobi et al., 1999; Moreira, 2001; Elustondo et al., 2002). This improvement

in terms of shrinkage may only be seen clearly when comparing the dried product obtained with that dried by a conventional atmospheric hot air drying.

As mentioned earlier, carrot that was dried at various temperatures but at the same pressure in LPSSD and vacuum dryer had similar values of the final volume and apparent density and similar degrees of shrinkage. Although it is known that the temperature directly affects the shrinkage property of the dried product because high temperature drying results in a higher moisture gradient within the material and so higher internal stresses, which leads to a larger degree of shrinkage, the effect of temperature on shrinkage was not indeed much significant in this case, both for the cases of LPSSD and vacuum drying. This is probably due to the fact that the differences in drying temperature used might not be large enough to cause significant differences in shrinkage. This is in accordance with the results of Ratti (1994) who also found that the shrinkage characteristics were independent of drying conditions over a limited range of drying temperature.

It should be noted, however, that although the values of shrinkage of carrot that underwent LPSSD and vacuum drying were similar, the shrinkage patterns resulted from the two different drying processes were quite different. Carrot that underwent vacuum drying tended to shrink non-uniformly. This characteristic is indeed rather typical of most food products (Potter and Hotchkiss, 1998). In a more rapid drying (as in the case of vacuum drying when compared with LPSSD) the surface of the drying product became dry and rigid long before the center had dried out; the center dried and shrank much later than the outer surface did and pulled away from the rigid surface layers and caused a non-uniform shrinkage. Drying carrot in LPSSD, however, led to a more uniform shrinkage; in this case shrinkage seemed to occur because the carrot structure could not support its own weight and hence collapsed under gravitational force in the absence of moisture (Achanta and Okos, 2000). This is because LPSSD offered a milder drying condition (since the drying chamber was moister than in the case of vacuum drying). Dense or rigid large formation might not as much be formed in the case of LPSSD as in the case of vacuum drying. The photographs of carrot cubes both after drying and after rehydration are shown in Figure 6

Regarding the rehydration ability of carrot undergoing both drying processes it can be seen in Table 2 that carrot that underwent LPSSD had much better rehydration capability than that vacuum dried. This is also due to the formation of dense layers in the case of vacuum drying, which led to non-uniform shrinkage mentioned earlier; the rather dense and rigid layers prevented the re-adsorption of water and hence led to lower degrees of rehydration. This can

also be seen from SEM photographs of Figures 7a and 7b, which show the microstructure of LPSSD and vacuum dried carrot, respectively. It is seen from these figures that carrot that underwent vacuum drying developed a rather dense layer and its pore distribution was rather non-uniform comparing with carrot that underwent LPSSD (see Figures 8a and 8b), which also did not have dense layer that prevented re-adsorption of water. It was also found that, in general, there existed an adverse relationship between the degree of rehydration and that of shrinkage.

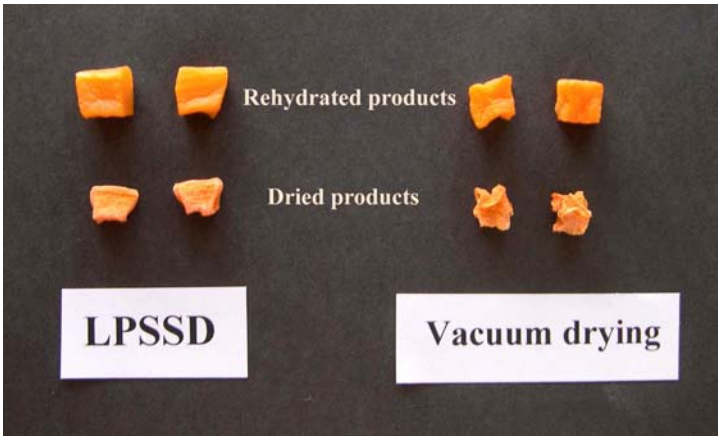

Figure 6. Photographs of carrot cubes both after drying and after rehydration

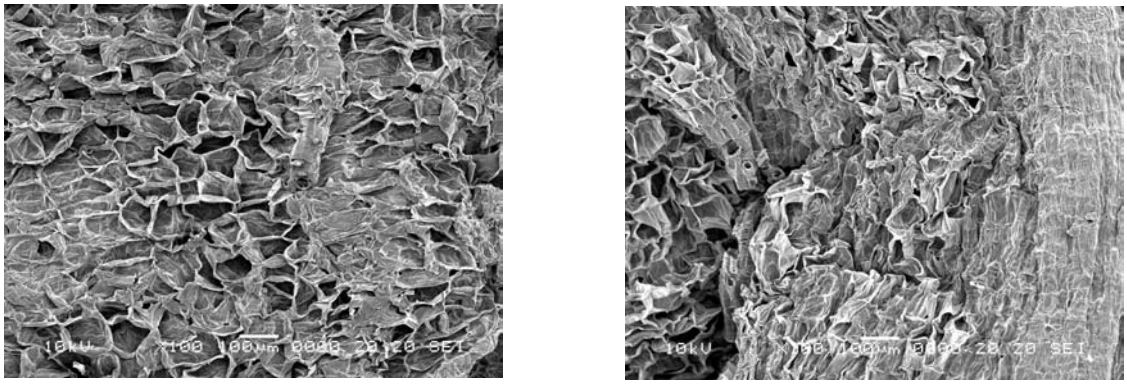

(a) LPSSD (b) Vacuum drying

Figure 7. SEM photographs of carrot undergoing

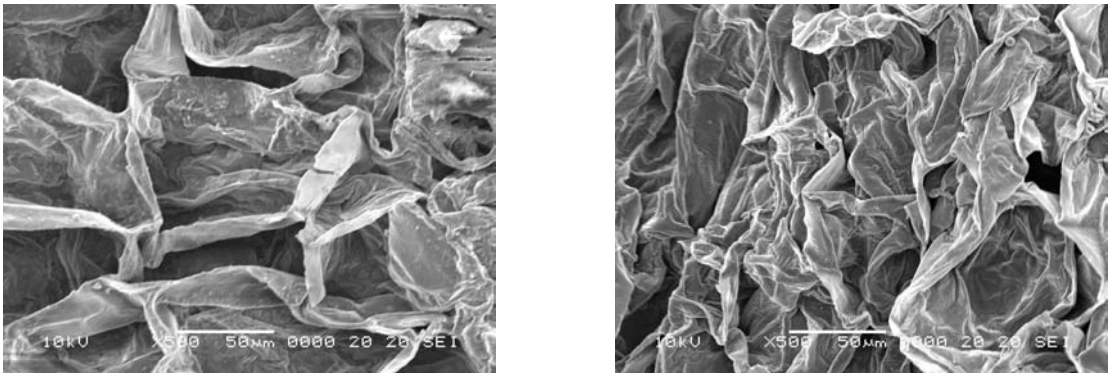

(a) LPSSD (b) Vacuum drying

Figure 8. SEM photographs showing pore distribution of carrot undergoing

The changes of color parameters (Δa and ΔL) of carrot undergoing LPSSD and vacuum drying are listed in Table 3. It was observed that all dried carrot was redder than fresh carrot as can be seen from the positive Δa values. On the other hand, it was observed that almost all drying conditions yielded dried carrot with negative ΔL values, which implied that the dried carrot was slightly darker than the fresh one.

It can be observed from Table 3 that, when comparing the effects of different drying methods that LPSSD yielded carrot of redder and lighter colors than those obtained by vacuum drying. These results were similar to those reported by Caixeta et al. (2002) who compared the color values of potato chips undergoing impingement superheated steam and hot air drying. It was found that lower drying temperatures gave redder and lighter dried carrot. This may be due to the fact that red color is attributed to the presence of β carotenes (Lin et al., 1998) and the degradation of β carotene in carrot is inversely proportional to the drying temperature (Pan et al., 1999). Operating pressure seems to have only a small effect on the colors of the dried carrot, however.

Table 3. Average values of Δa and ΔL of carrot undergoing LPSSD and vacuum drying at different operating conditions.

Drying Process	Temperature (°C)	Pressure (kPa)	Δa	ΔL
LPSSD	T = 60°C	7	0.2 ± 0.04^{e}	0.01 ± 0.02^{f}
		10	N/A	N/A
		13	N/A	N/A
	T = 70°C	7	0.17 ± 0.02^{d}	-0.04 ± 0.03^{e}
		10	0.16 ± 0.06^{d}	-0.04 ± 0.02^{e}
		13	0.16 ± 0.04^{d}	-0.04 ± 0.04^{e}
	T = 80°C	7	0.15 ± 0.01^{c}	-0.06 ± 0.08^{d}
		10	0.15 ± 0.01^{c}	-0.09 ± 0.17^{abc}
		13	0.15 ± 0.06^{c}	-0.08 ± 0.11^{cd}
Vacuum drying	T = 60°C	7	0.10 ± 0.02^{ab}	-0.05 ± 0.03^{de}
		10	0.10 ± 0.02^{ab}	-0.06 ± 0.03^{d}
		13	0.09 ± 0.02^{ab}	-0.1 ± 0.08^{ab}
	T = 70°C	7	0.07 ± 0.06^{a}	-0.09 ± 0.02^{a}
		10	0.07 ± 0.05^{a}	-0.1 ± 0.04^{ab}
		13	0.07 ± 0.1^{a}	-0.1 ± 0.03^{ab}
	T = 80°C	7	0.07 ± 0.01^{a}	-0.1 ± 0.06^{ab}
		10	0.07 ± 0.04^{a}	-0.1 ± 0.03^{ab}
		13	0.07 ± 0.07^{a}	-0.1 ± 0.02^{ab}

$^{a, b, c, d, e, f}$ in the same column with different superscripts means that the values are significantly different ($p<0.05$)

N/A implies that, at this condition, the final carrot moisture content of 0.07 kg/kg (d.b.) was not achievable

1.6 Conclusion

Detailed experimental evaluation of low-pressure superheated steam drying showed that, despite lower drying rates due to poorer convective heat transfer under reduced pressures, the process gave superior quality dried product compared to that obtained using conventional vacuum drying. It was observed that the effect of operating pressure was less significant than that of steam temperature. It is interesting to note that the operating pressure and temperature affected the shapes of the drying rate and temperature curves differently in steam drying and vacuum drying. The two drying techniques yielded differing structural and optical properties of the dried product. Steam drying provided better rehydration and a redder dried carrot than that obtained in vacuum drying over the operating parameter ranges studied.

Nomenclature

m_P = mass of an empty pycnometer, g

m_{Ph} = mass of a pycnometer filled with n-heptane, g

m_{Phs} = mass of a pycnometer with sample and n-heptane, g

m_s = masses of the sample, g

R = rehydration ratio, -

V = volume, cm^3

V_i = volume of fresh carrot, cm^3

Greek letters

ρ_{app} = apparent density, g/cm^3

ρ_h = density of n-heptane, g/cm^3

Module 2
Drying Rates and Inversion Temperature of a Low-Pressure Superheated Steam Drying System

2.1 Introduction

Based on the results of the first part (see Module 1) it was observed that the differences between the two sets of drying times (belonged to low-pressure superheated steam and vacuum drying) were smaller at higher drying temperatures. This suggested that raising the drying temperature further would eventually lead to equal rates of drying at the so-called inversion temperature (Mujumdar, 2000) due to increased temperature difference between the steam and the product as well as a reduction of the initial steam condensation. The information on inversion temperature of the low-pressure superheated steam drying system and the effect of vacuum pressure on this temperature was still missing, however. Although Shibata et al. (1988a, 1988b) have studied the steam drying mechanisms of sintered spheres of glass beads under atmospheric pressure and vacuum and reported that the drying mechanisms of the two processes were different and that superheated steam drying under vacuum gave lower critical moisture contents as well as higher drying rates in the falling rate period than those in air drying under vacuum, they have not reported any information about the inversion temperature of the systems.

2.2 Objectives

2.2.1 To investigate the effect of vacuum pressure on the value of inversion temperature when comparing the thin-layer drying rates of low-pressure superheated steam drying (LPSSD) and vacuum drying of model porous particles

2.2.2 To investigate and compare the values of the inversion temperatures calculated only from the rates of drying in the constant rate period with those calculated from the whole drying period

2.2.3 To develop a simple mathematical model that enables prediction of the product moisture content evolution

1.2.3 Experimental Set-up

See section 1.3

2.4 Material and Methods

Molecular sieve beads (Fluka, No. 69837), which had the pore size of 0.4 nm and an average diameter of 3.02 mm with the standard deviation of 0.34 mm and the bulk density of 750 kg/m^3 were used as the tested material in this part of the study. Prior to the start of each experiment, distilled water (6.7 g) was slowly but continuously sprayed on to the beads (22 g) to make the initial moisture content of the beads to be around 0.3 kg/kg (d.b.), which was roughly the maximum moisture holding capacity of the beads. The particles were then left in a tightly closed box at room temperature for about 5 hours to allow them to reach the equilibrium. The drying experiment was preformed by placing roughly 28.7 g of saturated particles (about 1000 beads) on the sample holder as a thin layer. The drying chamber was then sealed tightly and valve 2 was opened to allow the steam from the boiler to flow into the reservoir; the steam pressure was maintained at about 200 kPa (gage) in the reservoir. A vacuum pump was then switched on to evacuate the drying chamber to the desired operating pressure and the steam regulator was opened to slowly flash the steam into the drying chamber. Due to the low-pressure environment of the chamber the steam became superheated. An electric heater was used to maintain the steam temperature at the desired drying temperature. At the end of the drying process the break-up valve was opened to allow the air into the drying chamber before opening up the chamber door and loading off the sample.

The experiments were performed at the following conditions: steam absolute pressures of 7, 10 and 13 kPa; steam temperatures of 80°, 90° and 100°C. The flow rate of steam into the drying chamber was maintained at about 26 kg/h and the speed of the fan was fixed at 2100 rpm.

For vacuum drying experiments the same experimental set-up was used but without the application of steam to the drying chamber. The same operating conditions as those used for LPSSD were therefore achievable.

2.5 Results and Discussion

2.5.1 Drying characteristics

The drying curves of thin-layer porous particles undergoing LPSSD and vacuum drying at some selected conditions are shown in Figure 9. The drying curves of LPSSD at different conditions were quite different and the effect of temperature on the drying curves was greater than the effect of pressure, while the drying curves of vacuum drying at different conditions were rather similar. It is seen that the drying times of LPSSD at an operating temperature of 80°C were longer than those of vacuum drying for all operating pressures tested. However, the

drying times of both processes operated at 100°C were quite similar. This is due to the fact that increased drying temperature led to higher drying rates due to sharply increased temperature differences or gradients between the samples and the steam in the case of superheated steam drying. However, the temperature differences between the air temperature and the wet-bulb temperature of vacuum drying increased only slightly as the drying temperature increased. In addition, it can be observed that the equilibrium moisture contents of the beads underwent LPSSD were much higher than those underwent vacuum drying. For example, the equilibrium moisture contents of particles dried at 80°, 90° and 100°C using LPSSD at the operating pressure of 7 kPa were 1.5, 0.9 and 0.2% (d.b.), respectively, while the equilibrium moisture contents of particles were 0.09, 0.05, 0.02% (d.b.), respectively, in the case of vacuum drying at the same pressure. This led to increased humidity in the drying chamber of LPSSD and hence reduced the vapor pressure gradient, which is the driving force of the drying process. Therefore, the drying times of most LPSSD were higher than those of vacuum drying.

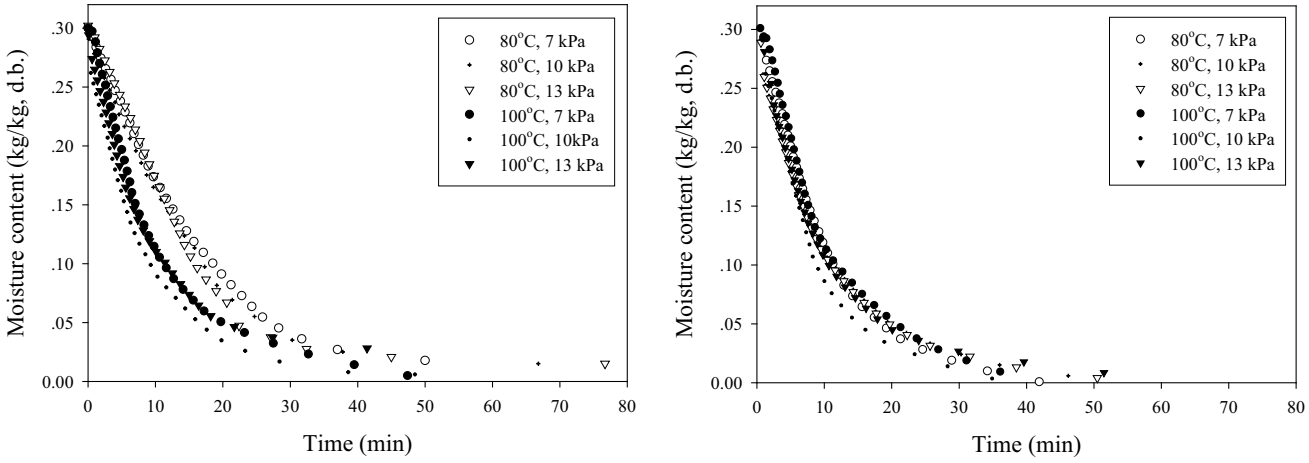

(a) LPSSD (b) Vacuum drying

Figure 9. Drying curves of molecular sieve particles

Figure 10 shows the comparison of the observed drying rate curves in superheated steam drying to those in vacuum drying at different operating conditions. For all conditions the drying rates slightly fluctuated but remained around the constant values as the moisture content decreased until the critical moisture content of each condition was reached. The drying rates then decreased continuously during the falling rate period (FRP). It can be seen from this figure that the critical moisture content was different for different conditions in the case of superheated steam drying (the critical moisture contents of particles dried, for example, at 80°,

90° and 100°C were 20, 17 and 15% (d.b.), respectively, at the operating pressure of 7 kPa) but were quite similar in the case vacuum drying (17% (d.b.) over the temperature range of 80°-100°C at the operating pressure of 7 kPa). It was also observed that the lower-pressure and higher-temperature superheated steam led to larger amount of water evaporation and also to higher critical moisture contents.

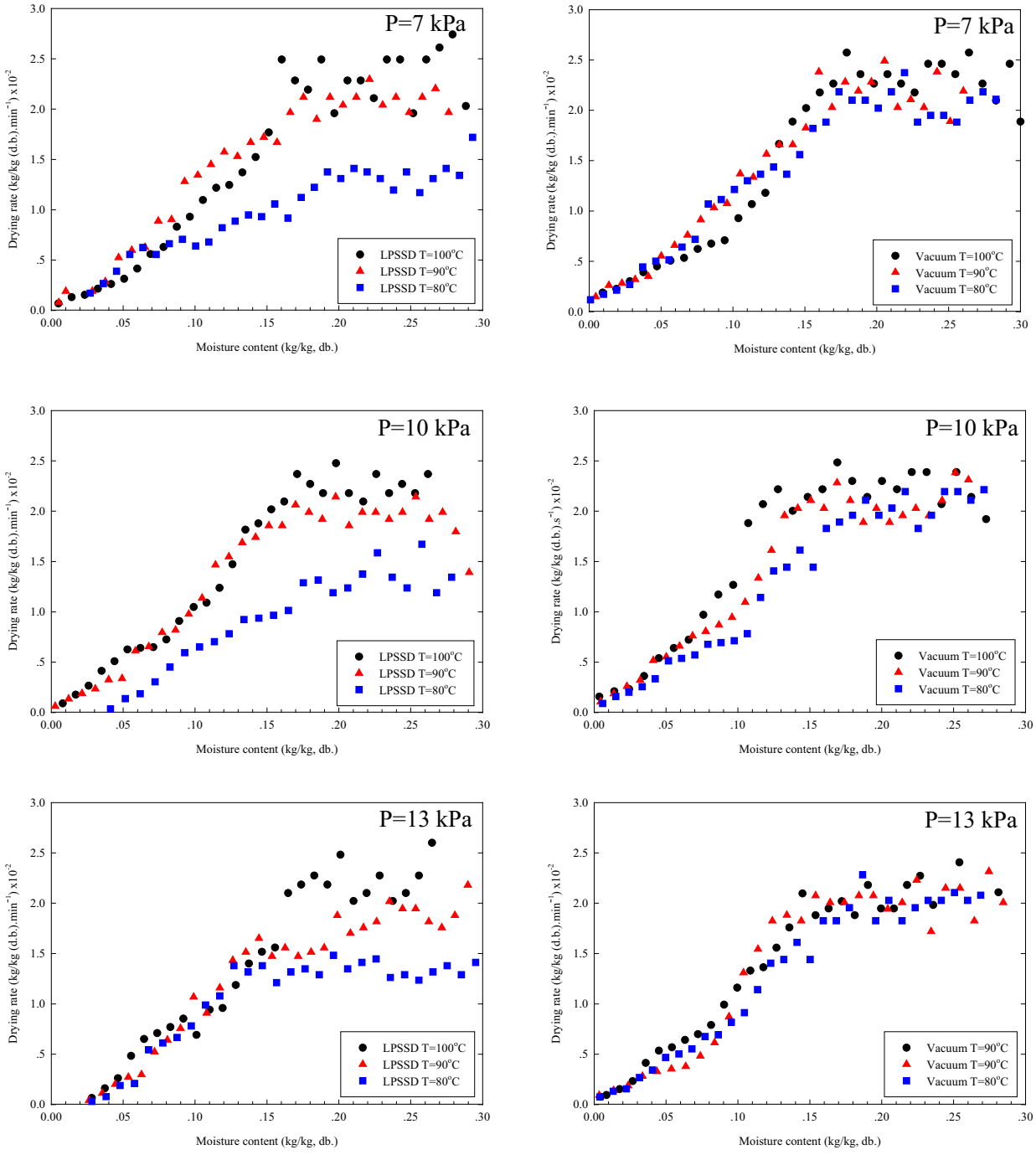

Figure 10. Drying rate curves of molecular sieve beads undergoing LPSSD and vacuum drying at various operating pressures

Figure 11 gives the rates of water evaporation during the constant rate period at various operating temperatures and pressures. It was found, as expected, that raising the drying temperature led to higher CRP drying rates due to increased temperature difference or gradient between the steam (or air) and the samples as well as a reduction of the initial steam condensation in the case of superheated steam drying. In the case of low-pressure superheated steam drying, the temperature difference was the difference between the superheated steam and saturation temperature at the corresponding operating pressure, while the temperature difference was the difference between the air temperature and the wet-bulb temperature (not saturation temperature since, in this case, the level of vacuum was not that high that the effect of convection by the fan could be negligible) in the case of vacuum drying. While the temperature differences (or driving force for heat transfer) of vacuum drying were higher at lower operating temperatures than those of low-pressure superheated steam drying, the values of the heat transfer coefficient were lower due to inferior thermal properties of air. Raising the drying temperature, however, led to higher temperature differences and hence higher CRP drying rates. The counter-acting effects of the heat transfer coefficient and the temperature difference led to inversion phenomenon, as shown also in Figure 11, where the CRP drying rates of vacuum drying and low-pressure superheated steam drying were equal. Beyond the inversion temperature the CRP drying rates of steam drying were higher than those of vacuum drying due both to the increased temperature difference and higher heat transfer coefficient.

When the operating pressure increased (at the same operating temperature) it can be seen that the evaporation rate was lower. This was due to the fact that the boiling temperature of water at higher pressure is higher; this led to decreased temperature difference and hence lower water evaporated rate.

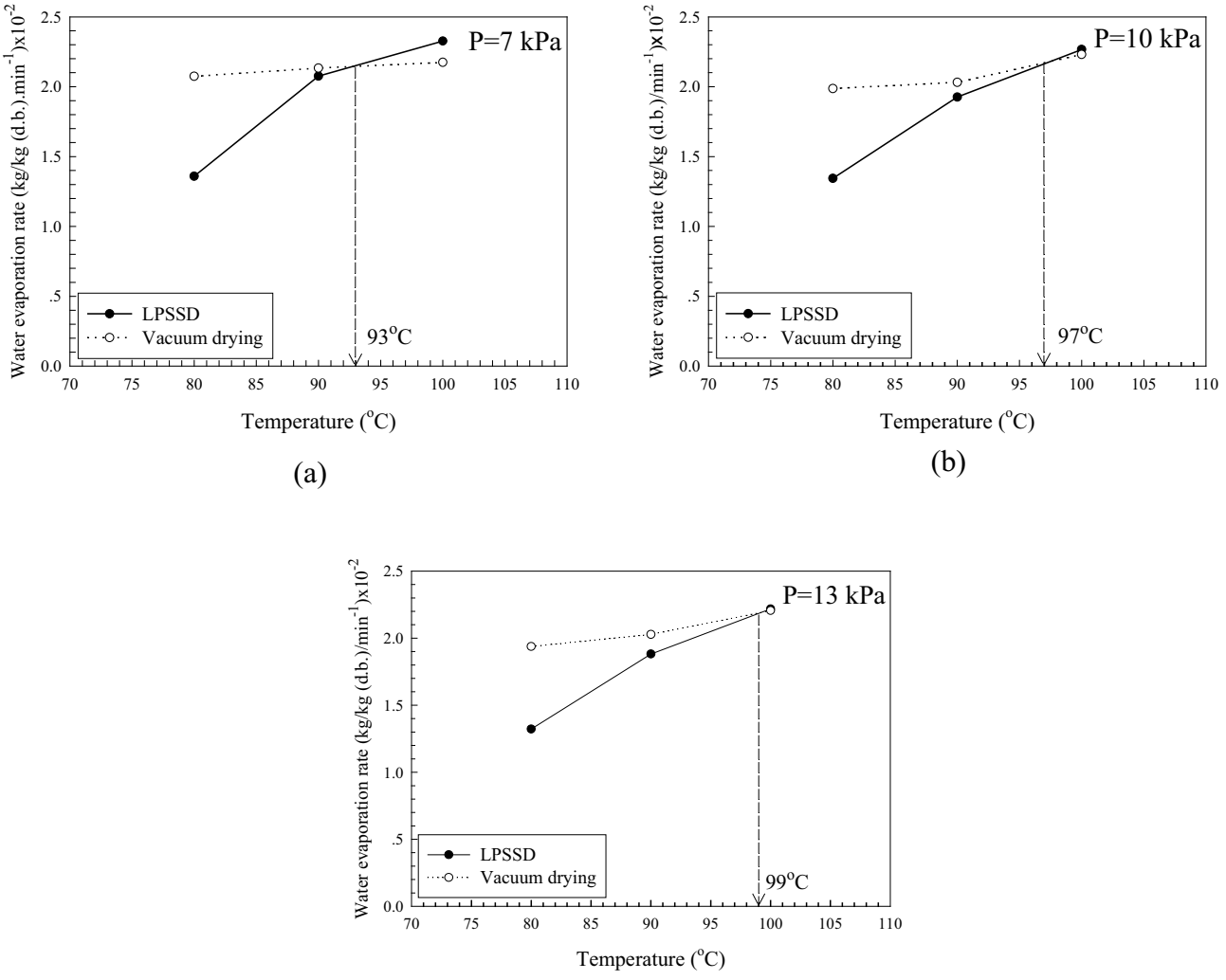

Figure 11. Constant-rate period evaporation rates of moisture from molecular sieve beads at various operating pressures

As mentioned earlier, the CRP drying rates depend on the rate of heat transfer and hence the difference between the surface temperature of the sample and the drying medium temperature. For this reason, the drying temperature had only a small effect on the rates of vacuum drying as compared with the case of low-pressure superheated steam dying since the wet-bulb temperature changes only slightly with increased drying temperature compared with the change of boiling temperature, especially at lower operating pressures.

2.5.2 Inversion temperature

Figure 12 shows the effect of operating pressure on the inversion temperature, which was calculated from the CRP rates (Figure 11). The inversion temperature at the operating pressure of 13 kPa was obtained by extending the plots of drying rates to the point where rates of vacuum and low-pressure superheated steam drying were equal. The data here confirm that the inversion temperature depends on the operating pressure and correlates almost linearly with it. This is because water at the surface of particles evaporates faster at lower pressures than at higher pressures because the difference between the boiling point and superheated steam temperature was higher as mentioned earlier. It is seen also from Figure 12 that when steam drying was performed at lower operating pressures (less than 7 kPa), its CRP drying rate would be higher than that of vacuum drying even at temperatures lower than 93°C. Using these conditions to operate the dryer would yield shorter drying times and this might preserve the quality of a heat-sensitive product better.

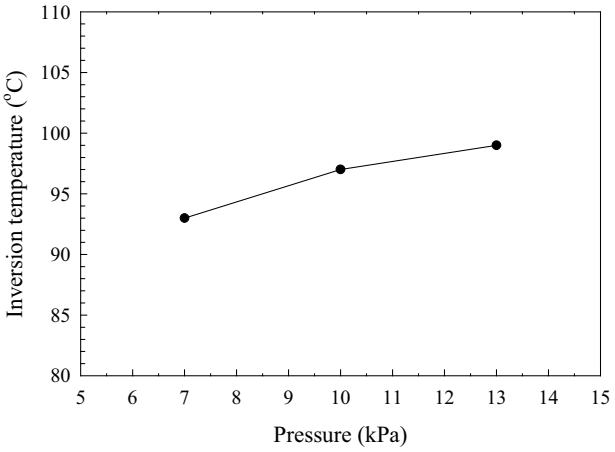

Figure 12. Effect of operating pressure on inversion temperature (based on CRP drying rates) of molecular sieve beads

Figure 13, on the other hand, shows the overall average drying rates calculated from combined constant rate period and falling rate period drying rates at various operating pressures. The intersection point was obtained by extending the plots of drying rates to the point where rates of vacuum and low-pressure superheated steam drying were equal. As mentioned earlier, the CRP drying rates depend only on external heat and mass transfer conditions since free water is always available for evaporation at the surface of the sample. However, in the FRP the rates depend not only on the rate of external heat transfer but more on the internal resistances to heat and mass transfer, which are somewhat material-dependent.

Therefore, the inversion temperatures calculated from combined CRP and FRP rates (or temperature at the intersection point, in the case where P = 7ka, 109°C) were not equal to those calculated from only CRP drying rates. It can also be seen from Figure 11 and Figure 13 that the differences between vacuum and steam drying CRP rates were greater than those between vacuum and steam drying calculated from combined CRP and FRP rates. This is due to the fact that in FRP the resistances to heat and mass transfer of superheated steam drying were lower than those of vacuum drying because the drying medium of steam drying was water. These effects of FRP drying rates therefore increased the values of the combined (or overall) drying rates of superheated steam drying and hence led to smaller differences between the overall drying rates of vacuum and steam drying.

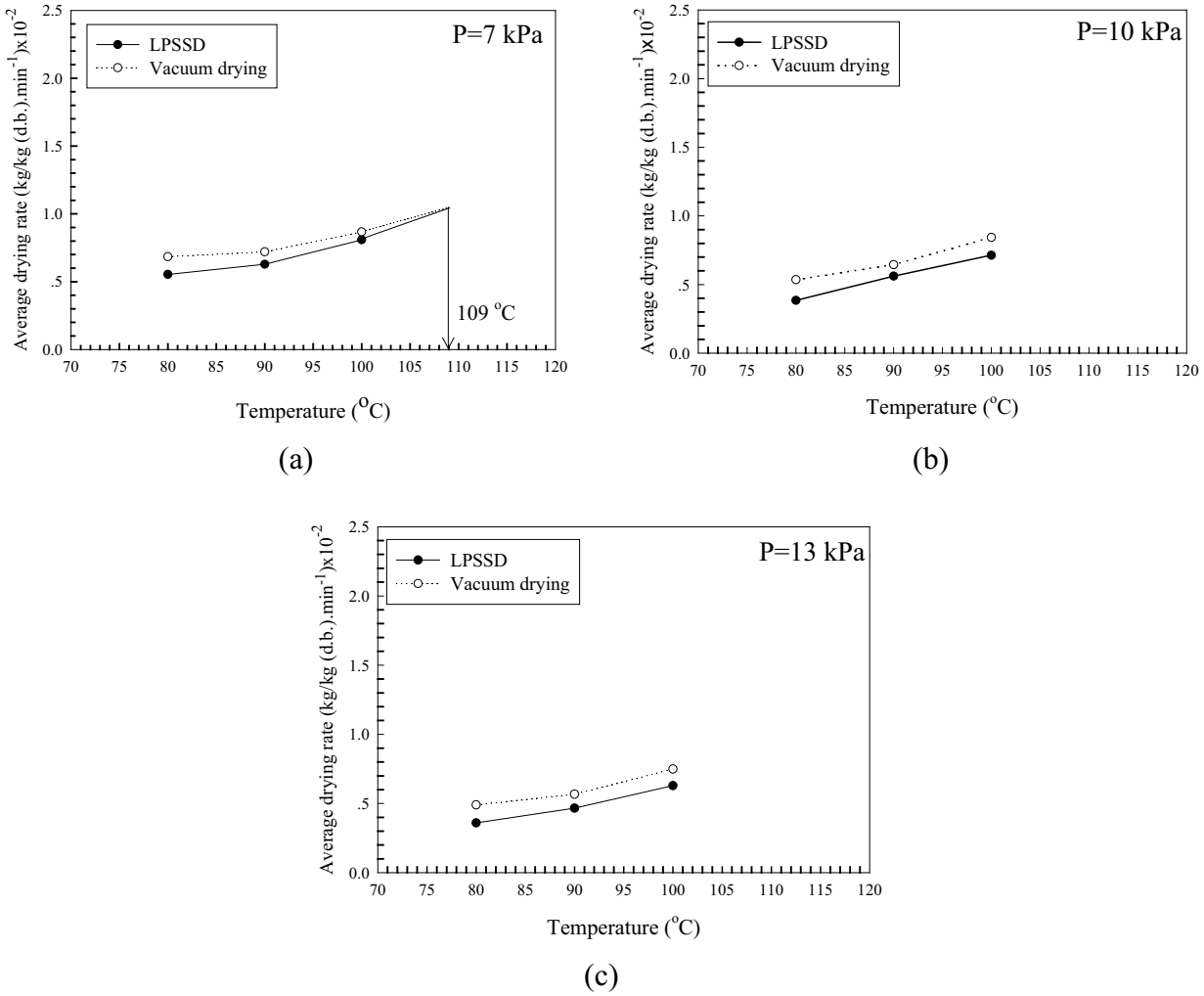

Figure 13. Average rate (CRP+FRP) of moisture removal from molecular sieve beads at various operating pressures

In addition, it can be seen from Figure 13(a) that the inversion temperature calculated from combined CRP and FRP rates (109°C) was higher than the inversion temperature calculated from only CRP rates (93°C) of Figure 11(a). This is because towards the end of FRP of low-pressure superheated steam drying the drying rates were lower than those of vacuum drying since the equilibrium moisture content of particles in low-pressure superheated steam environment was higher and hence there was a lower driving force for moisture transfer. This is ascribed to the fact that the drying chamber had higher humidity values than the drying chamber of vacuum drying. As mentioned earlier, the equilibrium moisture contents of particles dried using LPSSD were higher than those dried using vacuum drying (see Figure 9). At higher operating pressures (say, 13 kPa) the equilibrium moisture contents of particles dried in a low-pressure superheated steam dryer were even higher and these led to the reduction of the combined rates of drying of the low-pressure superheated steam drying. Therefore, at higher operating pressures the intersection points of equal rates of drying might not even be obtainable (see Figures 6(b), 6(c)).

2.5.3 Mathematical modeling

The equations were fitted with experimental data and the fitted equations were evaluated based on their R^2 and standard error of estimation. Comparing among three drying application models, the results show that Page's equation can predict the experimental data better than single-exponential equation and two-term exponential equation in the case of LPSSD, while single-exponential equation can predict the experimental data well in the case of vacuum drying at operating temperatures in the range of 80°-100°C and pressure of 7- 13 kPa as exemplified in Figures 14 and 15. The minimum R^2 of Page's equation was 0.997 and its maximum standard error of estimation was 0.0181 in the case of LPSSD while the minimum R^2 of single-term of exponential equation was 0.998 and its maximum standard error was 0.0233 in the case of vacuum drying. Drying constants of Page's equation (k and n) and of single-term exponential equation (a and b) depended on the operating drying temperature as well as the operating pressure.

Page's equation

$$MR = \frac{X_t - X_{eq}}{X_i - X_{eq}} = exp\left(-kt^n\right) \qquad (1)$$

The parameters k and n in the equation were determined from the experimental data and were correlated as follows:

For LPSSD

$$k = -2.39\times10^{-1} + 2.86\times10^{-3}\,T - 7.13\times10^{-3}\,P - 3.83\times10^{-6}\,TP + 5.42\times10^{-2}\,ln\,P \qquad R^2 = 0.95$$

$$n = 1.87 - 3.91\times10^{-3}\,T + 1.11\times10^{-1}\,P - 5.44\times10^{-4}\,TP - 4.35\times10^{-1}\,ln\,P \qquad R^2 = 0.86$$

For vacuum drying

$$k = -7.42\times10^{-2} - 7.07\times10^{-5}\,T - 1.01\times10^{-2}\,P + 1.22\times10^{-5}\,TP + 1.12\times10^{-1}\,ln\,P \qquad R^2 = 0.96$$

$$n = 1.12 - 2.40\times10^{-3}\,T - 7.88\times10^{-2}\,P + 4.92\times10^{-4}\,TP + 2.21\times10^{-1}\,ln\,P \qquad R^2 = 0.73$$

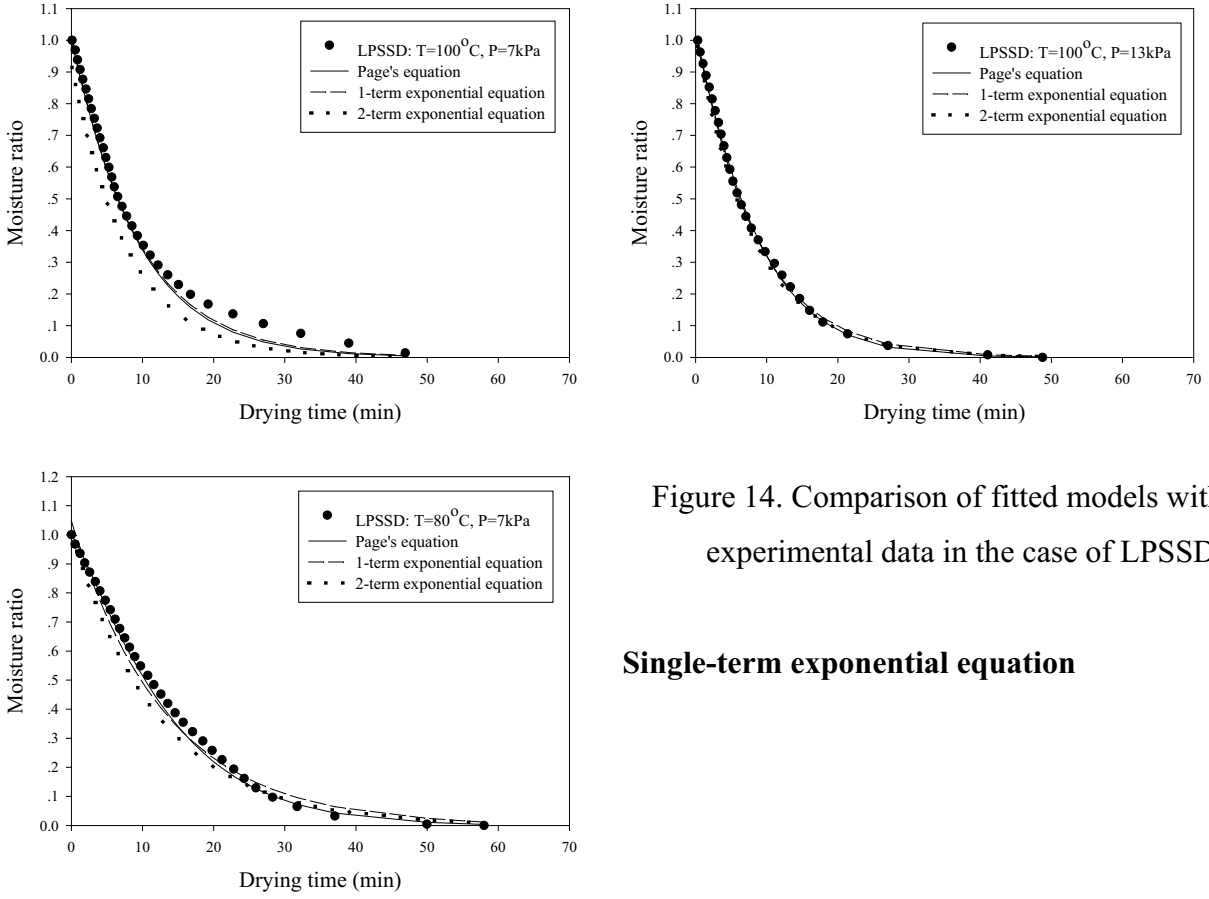

Figure 14. Comparison of fitted models with the experimental data in the case of LPSSD

Single-term exponential equation

$$MR = \frac{X_t - X_{eq}}{X_i - X_{eq}} = a\,exp\,(-bt) \qquad (2)$$

For LPSSD

$$a = 1.12 - 1.41\times10^{-3}\,T + 4.53\times10^{-3}\,P - 6.87\times10^{-6}\,TP + 6.53\times10^{-3}\,ln\,P \qquad R^2 = 0.75$$

$$b = -6.15\times10^{-2} + 1.12\times10^{-3}\,T - 9.75\times10^{-3}\,P + 7.56\times10^{-5}\,TP + 3.77\times10^{-2}\,ln\,P \qquad R^2 = 0.91$$

For vacuum drying

$$a = 9.68\times10^{-1} + 1.22\times10^{-3}\,T + 1.59\times10^{-4}\,P - 2.73\times10^{-5}\,TP - 1.12\times10^{-1}\,ln\,P \qquad R^2 = 0.94$$

$$b = 1.97\times10^{-2} - 3.74\times10^{-4}\,T - 2.13\times10^{-2}\,P + 1.08\times10^{-4}\,TP + 1.03\times10^{-1}\,ln\,P \qquad R^2 = 0.70$$

Two-term exponential equation

$$MR = \frac{X_t - X_{eq}}{X_i - X_{eq}} = a_1 \, exp\,(-b_1 t) + c_1 \, exp\,(-d_1 t) \qquad (3)$$

For LPSSD

$a_1 = \left(0.699 P^{-0.051}\right) exp\left(-51.312/T_{abs}\right)$ $R^2 = 0.62$

$b_1 = \left(354.576 P^{-0.0267}\right) exp\left(-2958/T_{abs}\right)$ $R^2 = 0.95$

$c_1 = \left(5.63 \times 10^{-3} P^{0.408}\right) exp\left(-1269.76/T_{abs}\right)$ $R^2 = 0.59$

$d_1 = \left(827.98 P^{-0.132}\right) exp\left(-3175.72/T_{abs}\right)$ $R^2 = 0.93$

For vacuum drying

$a_1 = \left(3.709 P^{0.554}\right) exp\left(-1056.055/T_{abs}\right)$ $R^2 = 0.53$

$b_1 = \left(0.164 P^{0.059}\right) exp\left(-185.677/T_{abs}\right)$ $R^2 = 0.49$

$c_1 = \left(1.63 \times 10^{-3} P^{-1.082}\right) exp\left(2773.12/T_{abs}\right)$ $R^2 = 0.75$

$d_1 = \left(4.73 \times 10^{-2} P^{-0.903}\right) exp\left(871.105/T_{abs}\right)$ $R^2 = 0.95$

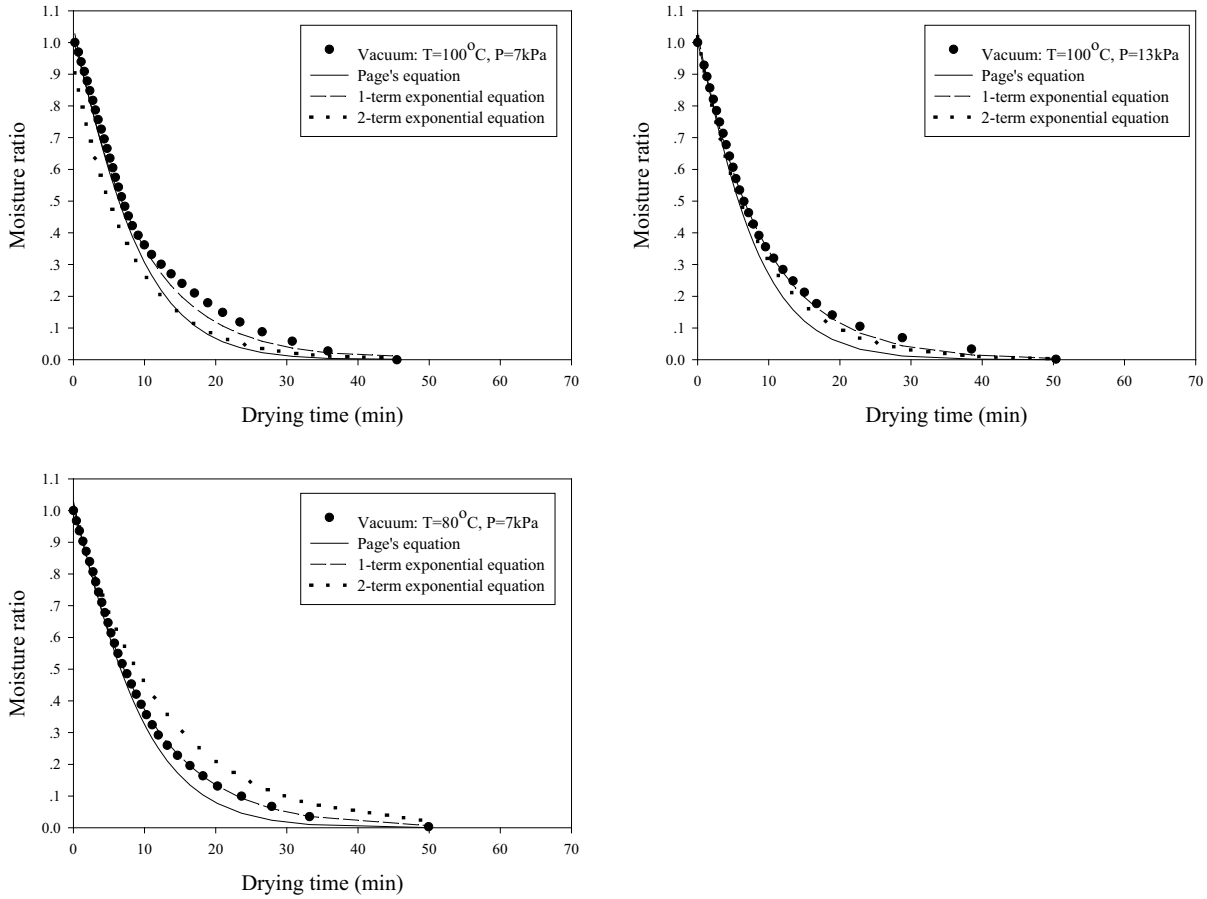

Figure 15. Comparison of fitted models with the experimental data in the case of vacuum drying

2.6 Conclusion

Effects of operating parameters, i.e., drying temperature and pressure, on the rates of vacuum and low-pressure superheated steam drying of model porous particles were experimentally investigated in this study. In addition, the values of the inversion temperature calculated only from the rates of drying in the constant rate period were compared with those calculated from the whole drying period (constant rate period and falling rate period) in order to point out the fundamental differences between the two sets of temperatures beyond which the drying rates in low-pressure superheated steam drying were higher than those in vacuum drying. It was found that the inversion temperatures calculated from combined CRP and FRP rates was higher than the inversion temperatures calculated from only CRP rates. At higher operating pressures the intersection points of equal rates of drying might not even be obtainable. The empirical models which can describe the experimental drying curves were also proposed. It was found that the Page's equation and single-term exponential equation can

predict well the experimental data of LPSSD and vacuum drying, respectively, over the ranges of operating temperature of 80-100°C and pressure of 7-10kPa.

Nomenclature

a	=	constant of single-term exponential model, -
a_1	=	constant of two-term exponential model, -
b	=	constant of single-term exponential model, -
b_1	=	constant of two-term exponential model, -
c_1	=	constant of two-term exponential model, -
d_1	=	constant of two-term exponential model, -
k	=	constant of Page's equation, -
MR	=	moisture ratio, -
n	=	constant of Page's equation, -
P	=	absolute pressure, kPa
t	=	drying time, min
T	=	temperature of drying medium, °C
T_{abs}	=	temperature of drying medium, K
X_{eq}	=	equilibrium moisture content, kg/kg, (d.b.)
X_i	=	initial moisture content, kg/kg, (d.b.)
X_t	=	moisture content at any time, kg/kg, (d.b.)

References

Achanta, S.; Okos, M.R. Quality Changes during Drying of Food Polymers. In *Drying Technology in Agriculture and Food Science*, A.S. Mujumdar, Ed.; Science Publishers, Inc.: Enfield, 2000; 133-147.

Caixeta, A.T.; Moraira, R.; Castell-Perez, M.E. Impingement Drying of Potato Chips. Journal of Food Process Engineering **2002**, 25(1), 63-90.

Devahastin, S.; Suvarnakuta, P.; Soponronnarit, S.; Mujumdar A.S. A Comparative Study of Low-Pressure Superheated Steam and Vacuum Drying of a Heat-Sensitive Material. [*In press*], Drying Technology **2004**.

Elustondo, D.; Elustondo, M.P.; Urbicain, M.J. Mathematical Modeling of Moisture Evaporation from Foodstuffs Exposed to Subatmospheric Pressure Superheated Steam. Journal of Food Engineering **2001**, 49(1), 15-24.

Iyota, H.; Nishimura, N.; Yoshida, M.; Nomura, T. Simulation of Superheated Steam Drying Considering Initial Steam Condensation. Drying Technology **2001**, 19(7), 1425-1440.

Krokida, M.K.; Maroulis, Z. Quality Changes during Drying of Food Materials. In *Drying Technology in Agriculture and Food Science*, A.S. Mujumdar, Ed.; Science Publishers, Inc.: Enfield, 2000; 61-106.

Krokida, M.K.; Oreopoulou, V.; Maroulis, Z.B. Modeling Shrinkage and Porosity during Vacuum Dehydration. International Journal of Food Science and Technology **1997**, 32(6) 445-458.

Li, Y.B.; Seyed-Yagoobi, J.; Moreira, R.G.; Yamsaengsung, R. Superheated Steam Impingement Drying of Tortilla Chips. In *Proceedings of the Eleventh International Drying Symposium (IDS'98),* Vol. B, Halkidiki, Greece, 1998; 1221-1228.

Lin, T.M.; Durance, T.D.; Scaman, C.H. Characterization of Vacuum Microwave, Air and Freeze Dried Carrot Slices. Food Research International **1998**, 31(2), 111-117.

Moreira, R.G. Impingement Drying of Foods Using Hot Air and Superheated Steam. Journal of Food Engineering **2001**, 49(4), 291-295.

Mujumdar, A.S. Superheated Steam Drying – Technology of the Future. In *Mujumdar's Practical Guide to Industrial Drying*, S. Devahastin, Ed.; Exergex: Brossard, Canada, 2000; 115-138.

Pan, Y.K.; Zhao, L.J.; Dong, Z.X.; Mujumdar, A.S.; Kudra, T. Intermittent Drying of Carrot in a Vibrated Fluid Bed: Effect on Product Quality. Drying Technology **1999**, 17(10), 2323-2340.

Ratti, C. Shrinkage during Drying of Foodstuffs. Journal of Food Engineering **1994**, 23(1), 91-95.

Seyed-Yagoobi, J.; Li, Y.B.; Moreira, R.G.; Yamsaengsung, R. Superheated Steam Impingement Drying of Tortilla Chips. Drying Technology **1999**, 17(1&2), 191-213.

Shibata, H.; Mada, J.; Shinohara, H. Drying Mechanism of Sintered Spheres of Glass Beads in Superheated Steam. Industrial & Engineering Chemistry Research **1988a**, 27(12), 2353-2362.

Shibata, H.; Mada, J.; Shinohara, H. Steam Drying of Sintered Glass Bead Spheres under Vacuum. Industrial & Engineering Chemistry Research **1988b**, 27(12), 2385-2387.

Tang, Z.; Cenkowski, S.; Muir, W.E. Dehydration of Sugar-beet Pulp in Superheated Steam and Hot Air. Transactions of the ASAE **2000**, 43(3), 685-689.

OUTPUT

1. Refereed Publications

Devahastin, S.; Suvarnakuta, P.; Soponronnarit, S.; Mujumdar, A.S. A Comparative Study of Low-pressure Superheated Steam and Vacuum Drying of a Heat-Sensitive Material. [*In press*], *Drying* Technology **2004**. **(Impact factor 0.58)**

Suvarnakuta, P.; Devahastin, S.; Soponronnarit, S.; Mujumdar, A.S. Drying Rates and Inversion Temperature of a Low-Pressure Superheated Steam Drying System. [Submitted], *Industrial and Engineering Chemistry Research* **2004**. **(Impact factor 1.25)**

2. Production of New Researcher

Some parts of this study constituted some parts of the doctoral thesis of Ms. Peamsuk Suvarnakuta, a D. Eng. student of the Department of Food Engineering, KMUTT.

3. International Conference

Suvarnakuta, P.; Devahastin, S.; Soponronnarit S.; Mujumdar, A.S. Drying Rates and Inversion Temperatures of Porous Particles Undergoing Low-pressure Superheated Steam and Vacuum Drying. In *Proceedings of the 15th International Symposium on Transport Phenomena,* Bangkok, Thailand, 2004.

Appendix 1

To appear in Drying Technology – An International Journal, 22(8), 2004

A COMPARATIVE STUDY OF LOW-PRESSURE SUPERHEATED STEAM AND VACUUM DRYING OF A HEAT-SENSITIVE MATERIAL

S. Devahastin[1,*], P. Suvarnakuta[1], S. Soponronnarit[2], A.S. Mujumdar[3]

[1]Department of Food Engineering, [2]School of Energy and Materials

King Mongkut's University of Technology Thonburi

91 Pracha u-tid Road, Bangkok 10140, Thailand

[3]Department of Mechanical Engineering, National University of Singapore

9 Engineering Drive, Singapore 117576

ABSTRACT

Using carrot cubes as a model heat-sensitive material, experimental investigations were conducted to examine the drying kinetics and various quality parameters of the dried product undergoing both low-pressure superheated steam and vacuum drying. Effects of operating parameters such as pressure and temperature on the drying characteristics as well as quality attributes, i.e., volume, shrinkage, apparent density, color and rehydration behavior, of the dried product underwent the two drying processes were also evaluated and compared. Although low-pressure steam drying required longer dwell time to achieve the same final moisture content than vacuum drying, some of the quality attributes were superior to those obtained in vacuum drying.

Keywords: apparent density, carrot, color, rehydration behavior, shrinkage, volume

[*] Corresponding author. Tel: +662 470 9246; Fax: +662 470 9240; e-mail: sakamon.dev@kmutt.ac.th

INTRODUCTION

During the past decade the idea of using superheated steam to dry food has been derived from other drying applications, e.g., paper drying (Mujumdar, 1981; Cui and Mujumdar, 1986; Douglas, 1994), coal drying (Potter, and Beeby, 1986), wood particles drying (Salin, 1986), sludge (Mujumdar, 1995) and pulp drying (Urbaniec and Malczewski, 1997; Tang et al., 2000). The notable advantages of superheated steam drying (SSD) that are of interest to food industry include the absence of oxidative reactions (e.g., enzymatic browning, lipid oxidation) due to lack of oxygen, high drying rates in both constant and falling rate periods, depending on steam temperature and pressure, and its ability to yield a higher porosity dried product due to an evolution of steam within the product. Moreover, SSD strips more of the acids that contribute to an undesirable taste or aroma of the products (Mujumdar, 2000).

Despite the many advantages of SSD as mentioned earlier, several limitations, especially when applying it to drying heat-sensitive materials like foods and bioproducts, are still present. Since most foods or other heat-sensitive products melt, undergo glass transition or are damaged at the saturation temperature of superheated steam corresponding to the atmospheric or higher pressures, one possible way to prevent the products from being damaged in a high-temperature environment of SSD is to operate a dryer at reduced pressure (Kumar and Mujumdar 1990; Mujumdar, 2000; Elustondo et al., 2001). Lowering the dryer operating pressure is a feasible option that not only preserves the quality of the dried product, but may also enhance the drying rate as well (Shibata et al., 1988; Shibata et al., 1990; Mujumdar, 2000; Senda et al., 2001; Elustondo et al., 2002). However, very little is reported on low-pressure (or sub-atmospheric) superheated steam drying of foodstuffs both from drying kinetics and dried product quality points of view.

Chen and Mujumdar (1989) performed a laboratory-scale testing of a sub-atmospheric pressure superheated steam drying of silk cocoons (at temperature around 45^{o}C) and found that this drying technique helped improving the quality of silk produced in terms of the brightness and

strength of fiber. The increased cost of steam drying was therefore justified by the additional credit received for the enhanced quality of the silk.

Pang and Dakin (1999) studied the drying rates and temperature profiles of stacks of softwood lumber undergoing vacuum SSD in a Moldrup kiln. The superheated steam temperature used was 90°C and had a circulating velocity of 10 m/s. Vacuum SSD was found to yield lower drying rates of whole lumber stack than those obtained using hot moist air. This is due to the fact that the wood temperatures in a vacuum SSD were lower than those used in hot air drying. However, the defects of the dried product such as kiln brown stain and drying stresses were lower. To reduce the drying time in a vacuum SSD, it was recommended that a higher steam circulating velocity (more than 10 m/s) be used.

Elustondo et al. (2001) studied sub-atmospheric pressure superheated steam drying of foodstuffs both experimentally and theoretically. Wood slabs, shrimps, bananas, apples, potatoes and cassava slices were dried using the steam pressures of 10,000-20,000 Pa, the steam temperatures of 60-90°C and the steam circulating velocities of 2-6 m/s. A semi-empirical mathematical model was also developed based on a theoretical drying mechanism, which assumed that the water removal was carried out by evaporation in a moving boundary allowing the vapor to flow through the dry layer built as drying proceeded to predict the drying characteristics of foodstuffs undergoing this drying operation. A simplified expression, which has two experimentally determined parameters, was derived and used to predict the drying rate of the tested samples. A model proposed was found to predict the drying kinetics reasonably well. No mention about the dried product quality is given, however.

The present work was therefore aimed at the design, fabrication and testing of a cabinet-type low-pressure superheated steam dryer and to investigate the influence of various operating parameters on the drying and heat transfer characteristics as well as various quality attributes of a heat-sensitive food product (carrot) undergoing this drying operation. Comparison was also made

with the similar sets of information obtained from vacuum drying experiments conducted in the same drying chamber.

EXPERIMENTAL SET-UP, MATERIALS AND METHODS

Experimental Set-up

A schematic diagram of the low-pressure superheated steam dryer and its accessories is shown in Figure 1. The dryer consists of a stainless steel drying chamber, insulated carefully with rock wool, with an inner dimension of $45\times\ 45\times 45$ cm^3; a steam reservoir, which received the steam from the boiler and maintained its pressure at around 200 kPa (gage); and a liquid ring vacuum pump (Nash, model ET32030, Germany), which was used to maintain the vacuum in the drying chamber. Steam trap was installed to reduce the excess steam condensation in the reservoir. An electric heater, rated at 1.5 kW, which was controlled by a PID controller (Omron, model E5CN, Japan) was installed in the drying chamber to control the steam temperature and to minimize the condensation of steam in the drying chamber during the start-up period; with the use of a heater the initial steam condensation during the start-up period was reduced considerably. A variable-speed electric fan was used to disperse steam throughout the drying chamber. The steam inlet was made into a cone shape and was covered with a screen to also help distribution of the steam in the chamber. The sample holder was made of a stainless steel screen with a dimensions of 12×12 cm^2. The change of the weight of the sample was detected continuously (at 30 seconds intervals) using a load cell (Minebea, model Ucg-3kg, Japan), which was installed in a smaller chamber connected to the drying chamber by a flexible hose (in order to maintain the same vacuum pressure as that in the drying chamber), and also to an indicator and recorder (AND A&D Co., model AD 4329, Japan). The temperatures of the steam and of the drying sample were also measured continuously using type K thermocouples, which were connected to an expansion board (Omega Engineering, model no. EXP-32, USA). Thermocouple signals were then multiplexed to a data acquisition card (Omega Engineering, model no. CIO-DAS16Jr., USA) installed in a PC.

LABTECH NOTEBOOK software (version 12.1, Laboratory Technologies Corp., USA) was then used to read and record the temperature data.

Materials and Methods

Fresh carrot was obtained from a local supermarket and stored at 4°C. Prior to the start of each experiment carrot was peeled and diced into 1 cm^3 cubes. To perform a drying experiment approximately 35 cubes of carrot (about 40 g) were placed on the sample holder. The drying chamber was then sealed tightly. Valve 2 was opened to allow the steam from the boiler to flow into the reservoir; the steam pressure was maintained at about 200 kPa (gage) in the reservoir. A vacuum pump was then switched on to evacuate the drying chamber to the desired operating pressure and the steam regulator was opened to slowly flash the steam into the drying chamber. Due to the low-pressure environment of the chamber the steam became superheated. An electric heater was used to maintain the steam temperature at a desired drying temperature. At the end of the drying process the break-up valve was opened to allow the air into the drying chamber (to regain an atmospheric condition) before opening up the chamber door and loading off the dried product.

For vacuum drying experiments the same experimental set-up was used but without the application of steam to the drying chamber. The same operating conditions were therefore achievable. The experiments were performed at the following conditions: steam absolute pressures of 7, 10 and 13 kPa; steam temperatures of 60°, 70° and 80°C. The flow rate of steam into the drying chamber (in the case of SSD) was maintained at about 26 kg/h and the speed of the fan was fixed at 2100 rpm.

Volume and apparent density measurements

The measurement of the sample volume (V) was performed using a liquid pycnometer with n-heptane as the working liquid. The apparent density (ρ_{app}) of the sample was also readily

obtained using this technique. The volume and apparent density of the sample were calculated according to the following equations:

$$V = \frac{\left[m_{Ph} - m_P\right] - \left[m_{Phs} - m_P - m_s\right]}{\rho_h} \quad (1)$$

$$\rho_{app} = \frac{weight\ of\ sample\ in\ air}{V} \quad (2)$$

where m_{Ph}, m_P, m_{Phs} and m_s are respectively masses of a pycnometer filled with n-heptane, empty pycnometer, pycnometer with sample and n-heptane, and mass of the sample. ρ_h is the density of n-heptane. The average values of five samples were reported. All measurements were performed in duplicate.

Shrinkage measurement

Five samples were used for a shrinkage measurement of each experimental condition. Shrinkage was expressed in terms of the percentage change of the volume of the original sample volume.

$$\%shrinkage = \frac{V_i - V}{V_i} \times 100 \quad (3)$$

where V_i and V are respectively the volumes of carrot at the beginning and at the end of each drying experiment. The average values of five samples were reported. All measurements were performed in duplicate.

Rehydration ability

The rehydration ratio (R) of the dried sample was determined by immersing dried carrot sample in hot water at 100^{o}C for 10 minutes. The sample was then drained and its volumes, both before and after immersion, were measured by a pycnometer. The rehydration ratio of the dried carrot was calculated by:

$$R = \frac{V_{after}}{V} \quad (4)$$

where V_{after} and V are respectively the volumes of dried carrot after and before immersion in hot water, respectively. The average valves of five samples were reported and all measurements were performed in duplicate.

Color measurement

Colors of the samples were measured in a Hunter Lab color system using a colorimeter (Juki, model JP 7100, Japan). For each drying experiment the color measurement was performed on five dried samples and the color values were compared with those of fresh samples. All experiments were performed in duplicate and the average values were then reported. The color changes (L and a values only) were calculated by:

$$\Delta L = \frac{L - L_i}{L_i} \quad \text{and} \quad \Delta a = \frac{a - a_i}{a_i} \quad (5)$$

where L and a represent the lightness and redness of the dried sample, respectively. L_i and a_i are respectively the lightness and redness of the fresh carrot sample.

All experimental data were analyzed using an analysis of variance (ANOVA). Tukey's test was employed to establish the multiple comparisons of mean values. Mean values were considered significantly different when $p<0.05$. From reproducibility tests the reproducibility values of the volume, density, percentage of shrinkage, rehydration ratio, Δa and ΔL were within ± 1.8%, 2.5%, 4.2%, 12.8%, 6.1% and 5.5%, respectively.

RESULTS AND DISCUSSION

Drying and heat transfer characteristics of carrot

After the low-pressure superheated steam dryer was fabricated it was tested to ensure that the distribution of the steam temperature within the drying chamber was uniform. It was found

from this study that the maximum difference of the steam temperature within the drying chamber was within ±3°C. The dryer was then used to conduct both low-pressure superheated steam drying (LPSSD) and conventional vacuum drying experiments.

Carrot that had an initial moisture content of about 9 kg/kg (d.b.) (or about 90% w.b.) was dried to a final moisture content of about 0.07 kg/kg (d.b.) (or about 6.5% w.b.) in the dryer using both low-pressure superheated steam and conventional vacuum drying. The drying curves of carrot undergoing LPSSD are shown in Figure 2; a slight decrease in the moisture content during the first 5 minutes of the process was due to the initialization of the chamber pressure and of the load cell. Drying indeed started at about 5 minutes after the weight was initially recorded. It can be seen in this figure that all samples gained a small amount of moisture during the first few minutes of drying (after the above-mentioned 5 minutes) for all drying conditions due to steam condensation. This phenomenon is indeed typical of superheated steam drying (e.g., Tang et al., 2000; Mujumdar, 2000) although, in this study, the drying chamber was preheated at 50°C during the first 5 minutes of the process. Nevertheless, the condensation of steam was rather negligible if the operating pressure was low; for example, the samples gained moisture of about 1.4%, 1.3% and 1 % when drying at 60°, 70° and 80°C at 7 kPa, respectively. Accordingly, the restoration time, which is the time by which the original mass has returned to its original value (Iyota et al., 2001) was 5, 4 and 4 minutes for drying at 60°, 70° and 80°C at 7 kPa, respectively.

Table 1 lists the drying times of all LPSSD and vacuum drying experiments. It can be seen from this table and also from Figure 2 that the effect of temperature on the drying rates was greater than the effect of pressure in the case of LPSSD, especially at higher drying temperatures. The effect of operating pressure was less clear even at lower temperature (60°C) for the case of vacuum drying, as can be seen in Figure 3, however. This may probably due to the fact that the steam thermal properties were affected by temperature to a larger extent than those of air, especially at lower drying temperatures. No initial condensation was also observed, as expected, in the case of

vacuum drying. It can also be seen that the moisture decreased faster at a higher temperature than at a lower temperature because the temperature difference between the sample and the medium at a higher drying temperature was greater than that at a lower temperature. For example, an increase of the drying temperature from 60°C to 80°C led to a reduction in the drying time of about 49% and 32% in the case of LPSSD and vacuum drying at an operating pressure of 7 kPa, respectively. In addition, it was observed that the moisture content decreased faster, especially in the case of LPSSD at lower drying temperatures, at lower pressures since water in carrot boiled and evaporated at lower temperatures; a decrease of the pressure from 13 kPa to 7 kPa, for example, led to a reduction of the drying time by 14% and 23% in the case of LPSSD and vacuum drying at a temperature of 80°C, respectively. Performing LPSSD experiments at higher pressures and lower temperatures also led to another problem, i.e., it was not able to dry carrot to the required moisture content of 0.07 kg/kg (d.b.) because there was an excessive amount of steam condensation in the drying chamber.

It was found that the drying times of vacuum drying were shorter than those of LPSSD (at the same pressure) for all conditions tested. This is probably due to the fact that the electric heater was used more often during vacuum drying since it was the only source of energy for drying. This might increase the amount of radiation absorbed by the carrot surfaces, thus explaining the higher drying rate during vacuum drying. The initial steam condensation on the product surface might also contribute to the longer drying times for the case of LPSSD. The differences between the two sets of drying times, however, were smaller at higher drying temperatures. Raising the drying temperature further would eventually lead to equal rates of drying at an inversion temperature (due to increased temperature difference between the steam and the product as well as a reduction of the initial steam condensation). This could not be done in this case, however, as it would adversely affect the quality of the dried carrot.

Figure 4 illustrates changes of moisture content and temperature of carrot undergoing LPSSD at some selected conditions. It can be seen in this figure that the shapes of the drying and temperature curves were affected by both the drying temperature and pressure. At lower drying temperatures (say, at 60°C and 70°C) the temperature of carrot changed suddenly from its initial value (after initial adjustment) and remained rather constant at the boiling temperature of water corresponding to the operating pressure until the first falling rate period drying ended (drying rate data are not shown here for the sake of brevity). Beyond this point, the carrot temperature rose again and finally approached the temperature of the drying medium. As the medium temperature increased (at the same operating pressure) it can be seen (for example, from Figure 4c) that the period of constant product temperature was shorter; the product temperature rose almost steadily from its initial value to the medium temperature. At the same drying temperature, however, increasing of the operating pressure led to a lower rate of drying but a longer period of constant product temperature (as can be seen from Figures 4c and 4d). It may depend both on the characteristics of the drying product and on these effects to determine the optimum operating conditions of an LPSSD.

Figure 5 shows the evolutions of moisture content and temperature of carrot undergoing vacuum drying at the same operating as those used for LPSSD shown in Figure 4. It can be seen from this figure that the drying and heat transfer behavior of carrot undergoing vacuum drying was quite different from that of LPSSD; the product temperature, in this case, rose almost steadily from its initial value to the medium temperature. However, the rates of moisture reduction in the case of vacuum drying were higher than those belonged to LPSSD, especially at lower drying temperatures as mentioned earlier.

Attempts were also made to compare the present data with a similar set of data available in the literature, i.e., the processes of freeze drying, air drying and microwave vacuum drying of carrot, in terms of the average drying rates over the whole period of drying (Lin et al., 1998). It

was found that the lowest drying rates obtained in the present study (which corresponded to using LPSSD at 60°C and 7 kPa) of 1.38 kg water kg^{-1} dry matter h^{-1} was, as expected, lower than that achievable by microwave vacuum drying (19.1 kg water kg^{-1} dry matter h^{-1}) but was still higher than those obtained by air drying and freeze drying of blanched carrot slices (1.31 and 0.013 kg water kg^{-1} dry matter h^{-1}, respectively). It should be noted that it is easier to dry blanched carrot than fresh carrot used in the present study. The carrot slices used by Lin et al. (1998) also had less thickness (4 mm) than that used in our study as well.

Volume, apparent density, shrinkage and rehydration behavior of carrot

Table 2 illustrates the effects of the drying temperature and pressure of both LPSSD and vacuum drying on various physical properties of carrot, i.e., volume, density, shrinkage and rehydration behavior. It was found that the volume of dried carrot was inversely proportional to its apparent density; carrot that had lower apparent density has larger volume, as expected. It can be seen also that the volume and apparent density of dried carrot undergoing both drying techniques slightly decreased and increased, respectively, as the operating pressure increased. This is due to the fact that pressure affects the percentage of air pores developed in the final dried products (Krokida and Maroulis, 2000); both properties changed only slightly in this case, however, because the narrow range of operating pressures tested. Different drying techniques as well as the drying temperature also did not have much effect on the volume and density of the final dried products in this case. This is in accordance with the results reported by Krokida et al. (1997) who compared the apparent density of dried carrot and other dried food products undergoing convective hot-air, microwave, freeze and osmotic drying; it was found in their work that the operating pressure significantly affected the apparent density of the dried products than did the other operating parameters. Lowering the pressure during subatmospheric drying (both LPSSD and vacuum drying) also helped preventing the structural collapse of foods, especially in the case of carrot.

Table 2 also shows the results of shrinkage of carrot undergoing different drying techniques and operating conditions. Like the apparent density, shrinkage values correlated directly with the volume of dried carrot. It can be seen from Table 2 that the percentage of shrinkage of LPSSD and vacuum dried carrot was similar although superheated steam drying is known to have a potential to reduce the degree of shrinkage of the drying product due to an evolution of vapor inside the product that expands into cells, leading to a normally porous dried product (Seyed-Yagoobi et al., 1999; Moreira, 2001; Elustondo et al., 2002). This improvement in terms of shrinkage may only be seen clearly when comparing the dried product obtained with that dried by a conventional atmospheric hot air drying.

As mentioned earlier, carrot that was dried at various temperatures but at the same pressure in LPSSD and vacuum dryer had similar values of the final volume and apparent density and similar degrees of shrinkage. Although it is known that the temperature directly affects the shrinkage property of the dried product because high temperature drying results in a higher moisture gradient within the material and so higher internal stresses, which leads to a larger degree of shrinkage, the effect of temperature on shrinkage was not indeed much significant in this case, both for the cases of LPSSD and vacuum drying. This is probably due to the fact that the differences in drying temperature used might not be large enough to cause significant differences in shrinkage. This is in accordance with the results of Ratti (1994) who also found that the shrinkage characteristics were independent of drying conditions over a limited range of drying temperature.

It should be noted, however, that although the values of shrinkage of carrot that underwent LPSSD and vacuum drying were similar, the shrinkage patterns resulted from the two different drying processes were quite different. Carrot that underwent vacuum drying tended to shrink non-uniformly. This characteristic is indeed rather typical of most food products (Potter and Hotchkiss, 1998). In a more rapid drying (as in the case of vacuum drying when compared with LPSSD) the